EFFECTS OF MEMBRANE LATERAL ORGANIZATION ON THE ANTICANCER ACTIVITY OF LIPOSOMAL CA4P AGAINST MCF-7 BREAST CANCER CELLS

A Dissertation
Submitted to
The Temple University Graduate Board

---

in Partial Fulfillment of the Requirements for the Degree
MASTER OF SCIENCE

---

by
Weiwei Zhu
May, 2010

ABSTRACT

Title: EFFECTS OF MEMBRANE LATERAL ORGANIZATION ON THE ANTICANCER ACTIVITY OF LIPOSOMAL CA4P AGAINST MCF-7 BREAST CANCER CELLS

Candidate's Name: Weiwei Zhu

Degree: Master of Science

Temple University, 2010

Master's Advisory Committee Chair: Parkson Lee-Gau Chong, Ph.D.

The goal of this research is to study how the cholesterol content in liposomal formulations affects the anticancer activity (e.g., cell growth suppression) of combretastatin A4 phosphate (CA4P). CA4P is a powerful antivascular agent currently under clinical trials for treating solid tumors. Liposomal CA4P has several advantages over free CA4P, including the reduced toxicities and the increased overall drug efficacy. In this thesis work, I have demonstrated that the proliferation of breast cancer MCF-7 cells varies with the cholesterol mole fraction in the formulation of liposomal CA4P in a biphasic manner, displaying a local minimum at the critical sterol mole fractions (C_r) for maximal superlattice formation. Cell proliferation was monitored using a fluorescence-based assay. Since cholesterol content determines membrane lateral organization, my results imply that membrane lateral organization plays an

important role in regulating the anti-cancer activity of liposomal CA4P. This finding provides a new concept in the rational design of liposomal anti-cancer drugs. More than 20 anticancer drug formulations are in the market or under clinical trials. Most of them include cholesterol as a major component. My present study indicates that cholesterol is not just serving as a vesicle stabilizing agent, but also modulates the activity of liposomal drugs. The principle learned from CA4P can be extended to other liposomal anti-cancer drugs. This study is also significant from the membrane biophysics point of view. The data provide additional support for the sterol superlattice model and illustrate that the concept of sterol superlattice can be applied to biotechnology development.

ACKNOWLEDGEMENTS

First, I would like to deeply thank my advisor Dr. Parkson Chong, who has provided me with a consistent support and mentoring both in science and in life throughout my graduate studies, and given me abundant opportunities to develop independence but yet always knew when to step in and offer guidance. Without his instruction, this thesis would not be possible.

I would like to thank all the members of the Chong lab with whom I worked closely and bonded daily, particularly Berenice Venegas Cotero, Ph.D. who taught me most of the bench technical skills and shared ideas about my research work; Dr. Michelle Olsher, who taught me how to strengthen my writing skills.

I would like to thank my student advisory committee members, Dr. Jimmy Collins and Dr. Salim Merali for always coming to offer me superb guidance and encouragement at committee meetings and provided useful comments into my work. Many other faculty members helped me along the way. I want to thank Dr. Danny Dhanasekaran, who gave me kindly support when I was the first year student at Temple University.

I would like to thank Dr. Marion Chan in the Microbiology Department for agreeing to serve on my thesis committee, Dr. Yuri Persidsky in the Pathology Department for allowing me to use the microplate reader, and Dr. Mohammad Kiani in the Mechanical Engineering Department for providing the anticancer drug CA4P.

Finally, I would like to thank my family who loves me immensely. I wish to extend the deepest gratitude to all of them.

TABLE OF CONTENTS

Page

LIST OF TABLES

LIST OF FIGURES

LIST OF ABBREVIATIONS

CA4	combretastatin A4
CA4P	disodium combretastatin A4 phosphate
Chol	cholesterol
DMPC	dimyristoyl-L-α-phosphatidylcholine
DPPC	dipalmitoyl-L-α-phosphatidylcholine
DSPE-PEG	distearoylphosphatidylethanolamine-polyethylene glycol
EDTA	ethylenediamine tetraacetic acid
Egg-PC	egg yolk phosphatidylcholine
EGTA	ethylene glycol-bis(b-aminoethyl ether)-N,N,N',N'-tetraacetic acid
LUVs	large unilamellar vesicles
MLVs	multilamellar vesicles
PBS	phosphate-buffered saline
PC	phosphatidylcholine
PEG	polyethylene glycol
PL	phospholipid
PLA_2	phospholipase A_2
POPC	1-palmitoyl-2-oleoyl-L-α-phosphatidylcholine
SPM	sphingomyelins
VDA	vascular disrupting agent

CHAPTER 1

INTRODUCTION

1.1 CA4 and CA4P

Tumor growth and metastasis require the development of new blood vessels (Mauer, et al., 2001). A single blood vessel can provide oxygen and nutrients for the survival of many tumor cells. Therefore, great efforts have been devoted to developing vascular disrupting agents (VDAs), which can cause the rapid and selective shutdown of the tumor vasculature, leading to tumor cell death (Maeda, et al., 2000).

Several low-molecular-weight VDAs, such as combretastatins, have generated much interest in this regard. Combretastatins are a series of stilbene compounds originally isolated from the South African bush willow tree *Combretum caffrum* (Pettit, et al., 1987). Combretastatin A4 (CA4, structure shown in Figure 1) is one of the most active among these stilbene compounds against tumor cells (Lin, 1988). CA4 and colchicines bear structure similarities (Figure 1). Colchicines are the well known VDAs. CA4 has been shown to bind to the β subunit of the tubulin at or close to the colchicine-binding site (McGown and Fox, 1989), but with even higher affinity (Straubinger, et al., 1985). Tubulin is a dimeric protein consisting of two subunits, α and β, of about 55,000 daltons. Tubulin makes up microtubule, which is one of the major components of the cytoskeleton. Microtubules are

structural units within cells and play a critical role in many important cellular processes such as cytoskeleton production, intercellular movement, cell movement, and formation of the mitotic spindle used in chromosome segregation and cellular division mitosis. A disruption of tubulin structure by VDAs, such as CA4 and colchicines, inhibits the formation of microtubules, consequently inhibiting cell proliferation.

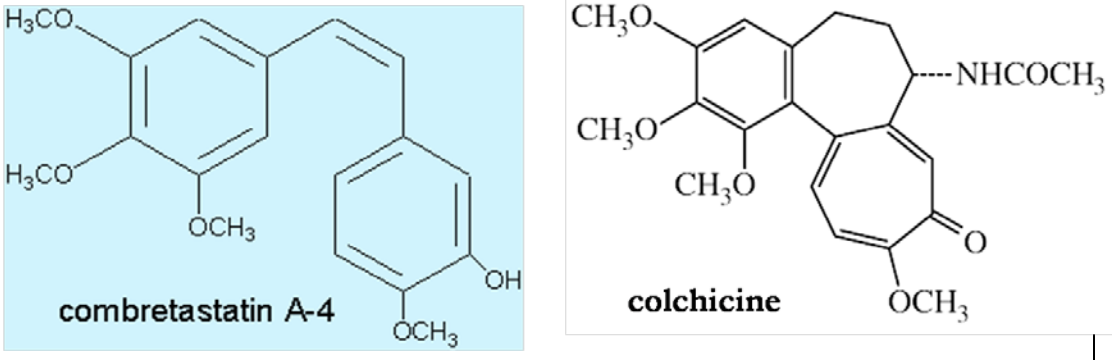

Figure 1. Chemical structures of combretastatin A4 (CA4) and colchicines.

An interesting feature of these VDAs is that, after administration, they have a preference to binding to tubulin in endothelial cells of tumor blood vessels, leaving normal tissues relatively intact. Thus, they cause a pronounced shutdown in blood flow to solid tumor, leading to extensive tumor cell necrosis (Galbraith, 2001, Grosios, et al., 1999). The antivasculature effect of CA4 (and its prodrug, discussed later) has been demonstrated both in animal models (Dark, et al., 1997a, Galbraith, et al., 2003, Tozer, et al., 1999) and human cancer patients (Anderson, et al., 2003, Rustin, et al., 2003, Stevenson, et al., 2003).

CA4 is much more clinically desirable than colchicines, even though both are potent VDAs. Colchicine is known for many years as a tubulin binding agent to have damaging effects on tumor vasculature. Like CA4, colchicine causes haemorrhage and extensive necrosis in both animal and human tumors (Algire, et al., 1954, Boyland and Boyland, 1937, Ludford, 1948, Seed, et al., 1940); however, colchicine is too toxic for clinical use. In contrast, the antivascular effects of CA4 were observed at well below their maximum tolerated doses in animal models. This difference has been attributed to the reversible binding kinetics of CA4 (McGown and Fox, 1989), as opposed to the pseudo-irreversible binding of colchicine itself (Lin, 1988, Lin, et al., 1989).

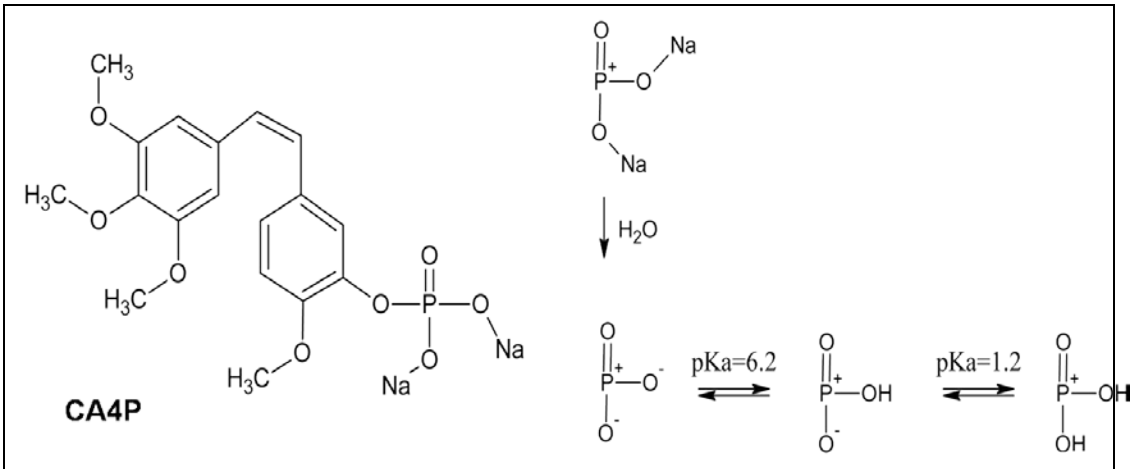

Figure 2. Structure of CA4P and the hydrolysis products of CA4P.

The development of CA4 has been progressing rapidly since the manufacture of a more water soluble sodium-phosphate salt, disodium combretastatin A-4 phosphate (CA4P, structure shown in Figure 2) (Pettit, et

al., 1987). Following administration, CA4P is rapidly cleaved to CA4 (Figure 2) by the action of endogenous non-specific phosphatases present in plasma and on endothelial cells. CA4P has been used as a prodrug of CA4, inducing vascular shutdown within tumors at doses less than one-tenth of the maximum tolerated dose (Dark, et al., 1997b). CA4P entered clinical trials in the United Kingdom and the United States in 1998. It is now in Phase II trials, in combination with conventional chemotherapy and radiotherapy, against a range of tumor types.

The initial *in vivo* studies demonstrated that CA4 reduced the tumor blood flow rate 24 hours after injection (Chaplin, et al., 1996). This experiment was carried out using the adenocarcinoma NT (CaNT) tumor grown subcutaneously in the rear dorsum of CBA/Gy f TO mice. Tumors were used when their geometric mean diameter was within the 6-8 mm range (Chaplin, et al., 1996). The study was then extended to the prodrug CA4P using the murine adenocarcinoma NT (CaNT), the human breast carcinoma MDA-MB-231, and the rat carcinosarcoma P22 (Dark, et al., 1997b). A single dose of 100 mg CA4P/kg caused 93% reduction in tumor vascular volume at 6 hours following drug administration and persisted over the next 12 hours, with extensive hemorrhagic necrosis (Dark, et al., 1997b). Due to blood vessel shutdown, acute hypoxiation occurred within 90 min following CA4P administration to rats bearing breast 13762NF tumors (Zhao, et al., 2005). Tozer's group, however, reported that, for a moderate dose of

CA4P in animal systems, a significant reduction in tumor blood flow can be detected within 5 minutes of drug administration and almost complete vascular shutdown can be obtained within 20 minutes (Tozer, 2001). It has also been shown that the combination of CA4P with the anticancer drug cisplatin or radiation caused enhanced growth delay, and cell death with no recurrence was achieved when CA4P was administered in a colorectal xenograft model (Chaplin, et al., 1999, Pedley, et al., 2001). In short, *in vivo* studies demonstrated that CA4 or CA4P reduced tumor blood flow rate on the order of minutes-hours after injection.

The most likely causes of the rapid collapse in tumor blood flow *in vivo* are morphological and functional changes associated with the endothelial cytoskeleton, similar to those that occur in endothelial cells *in vitro* within minutes of drug exposure. For example, proliferating human umbilical vein endothelial cells (HUVECs) round up when exposed to CA4P, and this is associated with condensation of the tubulin, reorganization of the actin cytoskeleton and increased permeability of the endothelial cell monolayer to macromolecules (Mayer, et al., 1997).

After treatment with CA4P, significant changes in cell shape (Galbraith, 2001), the assembly of actin stress fibers, actinomyosin contractility (Galbraith, 2001), formation of focal adhesions, disruption of cell-cell junctions, and monolayer permeability to macromolecules occur (Kanthou

and Tozer, 2002). An acute increase in tumor vascular permeability can result in several changes that function together to decrease blood flow.

Following treatment with CA4P, there is an upregulation of adhesion molecules, such as E-selectin, on the surface of endothelial cells (Brooks, 2003), which could help recruit neutrophils to tumors (Parkins, et al., 2000). This effect may also contribute to the vascular damaging and cytotoxic effects of CA4P.

CA4P is more cytotoxic to rapidly proliferating and immature endothelial cells than to quiescent mature cells (Sapra, et al., 2005). This differential effect allows for the selective effects of CA4P on tumor vasculature because there are much more proliferating or immature endothelial cells in tumor blood vessels than in normal vessels.

In addition to the microtubule-destabilizing effect, CA4P can inhibit the vascular endothelial-cadherin (VA-cadherin)/β-catenin/Akt signaling pathway, leading to regression of tumor neovessels (Vincent, et al., 2005).
VA-cadherin is an adhesion protein which is located exclusively at cell-cell contact regions of endothelium. VA-cadherin is involved in endothelial cell migration, survival, vascular integrity, and endothelial cell assembly into tubular structures. In other words, VA-cadherin supports the assembly of tumor neovessels. CA4P blocks assembly of tumor neovessels, thereby inhibiting tumor growth (Vincent, et al., 2005).

In this thesis work, I studied the effects of CA4P on the cultured breast cancer MCF-7 cell line, not in animals. Thus, CA4P was used not as a vascular disrupting agent. Rather, it was used simply as a tubulin-binding agent. Disruption of tubulin structure and microtubule formation by CA4P is sufficient to produce significant reduction in cell proliferation. MCF-7 breast cancer cell line was chosen because CA4P has been used to treat breast cancers and because previous studies have shown that CA4P inhibits MCF-7 cell growth (Hu, et al., 2007, Li, et al., 2005).

1.2 Liposomal CA4P

Despite its powerful tumor vascular disrupting activity and low toxicity compared to colchicines, CA4P has undesirable side effects in many normal tissues. Dose-related toxicities with CA4P have been detected in phase I clinical trials, which involved 34 patients with different tumor types (for examples, see Table 1). The most common problem was cardiotoxicity, with tachycardia occurred in 19 patients (53%), bradycardia in 8 patients (24%), and hypertension in 12 patients (35%) (Rustin, et al., 2003). These problems may be alleviated to a certain extent if liposomal CA4P is employed.

The advantages of using liposomal drugs opposed to free drugs have been well documented in the literature. Liposomes have been recognized as a useful drug delivery vehicle (Mauer, et al., 2001). Liposomes consist of an aqueous core entrapped by one or more bilayers of natural or synthetic lipids.

Liposomes composed of natural lipids are biodegradable, biologically inert, weakly immunogenic (Rooijen and Nieuwmegen, 1980), produce no antigenic or pyrogenic reactions and possess limited intrinsic toxicity (Campbell, 1983).

Table 1. Toxicities of CA4P.
Illustrations of toxicities of CA4P detected in Phase I clinical trials. The figures indicate the numbers of patients showing the specified symptoms from a group of 34 individuals. [modified from (Rustin, et al., 2003)]

Side effects	Dose Level			
	5-40 mg/m^2	52 mg/m^2	68 mg/m^2	88-114 mg/m^2
Tachycardia	0	5	4	10
Bradycardia	0	1	2	5
Hypertension	1	2	3	6
Tumor Pain	1	4	2	4
Headache	1	1	4	2
Vomiting	0	1	2	4

Drugs with varying structures can be encapsulated in liposomes either in the lipid bilayer, in the interior aqueous core or at the bilayer interface. Reformulation of liposomal drugs can change the biodistribution of liposomes in animals. Liposomal drugs allow higher drug dosage and less frequent drug administration. Reformulation may be used as a strategy to enhance the efficacy of various therapeutic agents. Liposomes can be tailored to control retention of entrapped drugs in biological fluids and to

enhance liposomal drug uptake by target cells (Gregoriadis and Florence, 1993). Drugs encapsulated in liposomes are expected to be transported without significant degradation and with minimum side effects to the recipients.

Great efforts have been made to develop strategies for targeted delivery to specific organs, cells or compartments within the cells (Gregoriadis, 1977). Liposomes are well suited for targeted delivery because of the ease of modifying their surface when compared with other drug carriers such as nanoparticles (Grislain, et al., 1983, Illum, et al., 1983) and microemulsions (Hashida, et al., 1977, Mizushima, et al., 1982). Many approaches have been attempted to achieve targetable properties, including noncovalent association of cell specific antibodies with liposomes (Gregoriadis and Neerunjun, 1975), coating of liposomes with heat aggregated immunoglobulins M (IgM) (Weissmann, et al., 1975), covalent attachment of poly- and mono-clonal antibodies to the liposomes (Koning, et al., 2002, Moribe and Maruyama, 2002), glycoprotein bearing liposomes (Banuo, et al., 1983), and glycolipid containing liposomes (Soriano, et al., 1983, Wu, et al., 1982). The compounds entrapped into the liposomes are protected from the action of external media, particularly enzymes (Chaize and Colletier, 2004) and inhibitors. Moreover, liposomes allow the drugs to be delivered into cells by fusion or endocytosis mechanism and practically any drug can be entrapped into liposomes irrespective of its solubility.

Liposomal drugs display some unique pharmacokinetic characteristics partly due to their sizes, which typically range from 50 to 250 nm in diameter. These nano-scaled liposomes can be cleared from the body via the reticuloendothelial system, resulting in a relatively long systemic circulation time. Very often, liposomes distribute favorably to the liver and spleen as well as the site of solid tumors due to increased endothelial permeability and reduced lymphatic drainage in these tissues (Maeda, et al., 2000). Liposomal delivery is therefore a means to modify the pharmacokinetic and pharmacodynamic properties of therapeutic agents. Such modifications can improve the therapeutic efficacy of anticancer drugs and reduce their toxicities. For example, long circulating polyethylene glycol (PEG)-coated liposomal formulation of doxorubicin has been shown to exhibit increased solid tumor accumulation due to the enhanced permeability and retention effect and decreased dose-limiting cardiac toxicity relative to the free drug (Gabizon, et al., 2003).

Liposomal CA4 and liposomal CA4P have been developed and tested in animal models by Kiani's group in the Mechanical Engineering Department at Temple University, in collaboration with our laboratory (Pattillo, et al., 2005, Pattillo, et al., 2009). The animal studies (Pattillo, et al., 2005, Pattillo, et al., 2009) showed that liposomal CA4P holds great promises as an antivascular agent to treat solid tumors; those studies were carried out using the following CA4P liposomal formulations:

HSPC:cholesterol:DSPE-PEG (50:45:5 mol%). HSPC stands for hydrogenated soy phosphatidylcholine and DSPE-PEG for distearoylphosphatidylethanolamine-polyethylene glycol. Those liposomes carried ligands (antibodies) to radiation induced upregulated adhesion molecules on their surfaces. Those immunoliposomes would be preferentially distributed to the irradiated tumor region thereby circumventing the undesirable side effects of CA4P on normal tissues. Targeting of CA4P to irradiated mice bearing transplanted MCa-4 mouse mammary tumors via ligand-bearing HSPC/chol/DSPE-PEG liposomes (formulation shown above) resulted in significant tumor growth delay compared to all other treatment groups such as free CA4P, tumor radiation alone, liposomal CA4P alone and empty liposomes (Pattillo, et al., 2005, Pattillo, et al., 2009).

1.3 Incorporation of cholesterol into liposomal CA4P formulations

Lipid composition determines the physicochemical properties of liposomes (Chonn, et al., 1992). Damen et al. demonstrated that incorporation of cholesterol (CHOL), by causing increased packing of phospholipids in the lipid bilayer, reduces transfer of phospholipids to high density lipoproteins (HDL) (Damen et al., 1981). Senior et al. demonstrated that liposomes obtained from phosphatidylcholine (PC) with saturated fatty acyl chains (with a high liquid crystalline transition temperature) or from

sphingomyelin (SPM) are more stable in the blood than liposomes prepared from PC with unsaturated fatty acyl chains (Senior, 1982). Lipid composition in liposomal membranes should affect the drug release from liposomes and the overall efficacy of the entrapped drugs.

Table 2. Lipid compositions in liposomal anticancer drugs.

Active agent (product name)	Composition	Active agent (product name)	Composition
DaunoXome® (daunorubicin)	DSPC/CHOL	MBT-0206 (paclitaxel)	DOPE/DO-trimethylammoniumpropane
DOXIL®/Caelyx® (doxorubicin)	SoyHPC/CHOL/DSPE-P	OSI-211 (lurtotecan)	SoyHPC/CHOL
Myocet®/Evacet® (doxorubicin)	EPC/CHOL	Marqibo® (vincristine)	DSPPC/CHOL/sphingosine
SPI-077 (cisplatin)	SoyHPC/CHOL/DSPE-P	Atragen® (t-retinoic acid)	DMPC, and soybean oil
Lipoplatin™ (cisplatin)	SoyPC/DPPG/CHOL	INX-0125 (vinorelbine)	DSPPC/CHOL/sphingosine
S-CKD602 (camptothecin analog)	—	INX-0076 (topotecan)	DSPPC/CHOL/sphingosine
Aroplatin (oxaliplatin analog)	DMPC/DMPG	Liposomal-Annamycin®	DSPC/DSPG/Tween
Depocyt	DOPC/DPPG/CHOL/tr	Ambisome® (amphotericin)	SoyHPC/DSPPC/CHOL
LEP-ETU (paclitaxel)	DOPE/CHOL/cardiolipi	Nyotran® (nistatin)	DMPC/DMPG/CHOL
LEM-ETU (mitoxantrone)	DOPE/CHOL/cardiolipi		

In the study of Pattillo et al. (Pattillo, et al., 2009), cholesterol (45 mol%) was a major component in the liposomal CA4P formulation. In fact, cholesterol is often used as a major component in the formulations of many liposomal drugs. For example, to date, more than 20 liposomal anticancer drugs are on the market or under clinical trials. About 75% of them use cholesterol as a major lipid component (see Table 2 for examples). The traditional thinking is that cholesterol can cause a condensing effect on

membranes, thus increasing liposome stability in circulation and other tissues and consequently increasing the efficacy of the drug. For example, a doxorubicin liposomal formulation (US patent 4898735) contained 20-50 mol% cholesterol, 10-40 mol% negatively charged phospholipids, 2.5 mol% doxorubicin (lipid soluble), 0.2 mol% alpha-tocopherol (as an antioxidant), and some phosphatidylcholine (PC). It was claimed in the above-mentioned patent that 20 mol% cholesterol caused a 2-3 times increase in drug retention, but no additional improvement was seen up to 50 mol% cholesterol. It appears that cholesterol has been recognized as a useful stabilizing agent in liposomal drug formulations and that this has been the only known function of using cholesterol in liposomal anticancer drug formulations.

1.4 Importance of cholesterol content in liposomal Drugs

The cholesterol content in the CA4P liposomal formulation used by Pattilo et al. was 45 mol% (Pattillo, et al., 2009). This value was chosen arbitrarily, not based on a systematic study or a logical design. With regard to the optimal cholesterol content in liposomal CA4, there was an earlier report from Kiani's group comparing different liposomal formulations (Nallamothu, et al., 2006). It was claimed that 30 mol% cholesterol is optimum for maximal CA4 loading and its minimal leakage (Nallamothu, et al., 2006). Note that their data came from CA4, not from the water soluble

form CA4P and that their data were very limited (Nallamothu, et al., 2006). They examined only three formulations: HSPC/cholesterol/DSPE-PEG (65/30/5 mol%); HSPC/cholesterol/DSPE-PEG (95/0/5 mol%); HSPC/cholesterol/DSPE-PEG (62.5/30/7.5 mol%) (Nallamothu, et al., 2006).

We believe that the cholesterol content in liposomal drugs is not a trivial issue and that a much more detailed cholesterol study is needed. More importantly, the previous study of this kind is totally empirical; there was no theory providing a rational selection of optimal cholesterol content for liposomal drugs. My study aims to remedy these problems. I will first describe our theory and hypotheses of how cholesterol content should affect liposomal drug activities. Then, I will use more than 30 different formulations to test our hypotheses. Third, I will focus on CA4P rather than CA4 because CA4P is water soluble with higher efficacy in anticancer activity.

1.5 Cholesterol content and membrane lateral organization

Cholesterol content changes membrane properties via changes in membrane lateral organization. This is a key concept involved in this thesis work. As mentioned earlier, cholesterol (due to its unique rigid and flat structure) causes a condensing effect on neighboring fatty acyl chains in fluid lipid bilayers; therefore, cholesterol helps to stabilize liposomes in the blood and other tissues. It would be a common hypothesis that an increase of cholesterol content in the membrane will increase the condensing effect of

cholesterol on liposomal membranes, thus reducing membrane free volume with increasing cholesterol content in a monotonic manner. However, in many experiments, it was found that membrane free volume varied with membrane cholesterol content in a biphasic manner (rather than a monotonic manner) (Chong, 1994, Chong, 1996, Chong and Olsher, 2004). The biphasic behavior occurs at specific cholesterol mole fractions such as 20.0, 22.2, 33.3, 40.0 and 50.0 mol% sterol in diacyl-phosphatidylcholines. How can we understand this rather counter-intuitive observation?

This biphasic behavior can be explained by the sterol superlattice model (Chong, et al., 1994, Tang and Chong, 1992, Virtanen, et al., 1988). According to this model, cholesterol can be regularly distributed in lipid membranes. This sterol regular distribution (e.g., sterol superlattice) model (Figure 3) proposes that cholesterol can be organized in a regular lattice within the matrix lattice formed by membrane phospholipid acyl chains and sterol molecules. Regularly distributed sterol superlattices (shaded areas, Figure 3) and irregularly distributed lipid areas (blank areas, Figure 3) always coexist in fluid sterol-containing membranes (rectangle-like objects, Figure 3), with the ratio of irregular to regular regions (R; solid line in the bottom diagram of Figure 3) reaching a local minimum at critical sterol mole fractions (C_r) (*e.g.*, 20.0, 22.2, 25.0, 33.3, 40.0, & 50.0 mol% sterol). The C_r values can be calculated from the superlattice theories (Chong, 1994, Chong, et al., 1994, Tang and Chong, 1992). The model further proposes that the shape

and size of the regular regions fluctuate with time, and lipids inside and outside the regular regions undergo constant exchanges.

In the regular regions, sterol molecules (dark circles, Figure 3) are distributed into either hexagonal or centered rectangular superlattices. Additionally, in the regular region, lipid packing is tight, thus, possessing little membrane free volume. Since the ratio of irregular-to-regular regions reaches a local minimum at C_r values, membrane free volume (V; solid line in the bottom diagram of Figure 3) also varies with cholesterol content in a biphasic manner at C_r.

The perimeter of the regular regions is proportional to the size of the regular regions. Thus the perimeter (P; dashed line in the bottom diagram of Figure 3) of the regular regions may increase abruptly at C_r causing a large increase in the interfacial area between the regular and irregular regions, making sterols at C_r more exposed to the aqueous phase than sterols at non-C_r. The interfacial regions are not well packed. Through the interfacial regions, the entrapped CA4P molecules should leak out of the liposomes more and faster. Since the interfacial regions reach a local maximum at C_r, CA4P should exhibit its highest *in vitro* anti-microtubule effect when the cholesterol content in liposomal formulation is at C_r.

1.6 Hypotheses

Based on this theory, we hypothesize that when cancer cells are treated with liposomal CA4P, cell proliferation rate changes with cholesterol content in liposomal CA4P in a biphasic manner, reaching a local minimum at critical sterol mole fraction C_r for maximal superlattice formation. Since there are a few C_r values in the cholesterol mole fraction range 18-52 mol%, the variation of cell proliferation rate with liposomal cholesterol content should be multiple biphasic, instead of single biphasic.

I have tested these hypotheses using MCF-7 breast cancer cells and Chol/POPC LUVs containing CA4P. The key of the experimental design was to use small cholesterol increments (e.g., 0.5 mol% cholesterol) over a wide range of cholesterol mole fractions. Only in this way can biphasic changes in cell proliferation at C_r be detected.

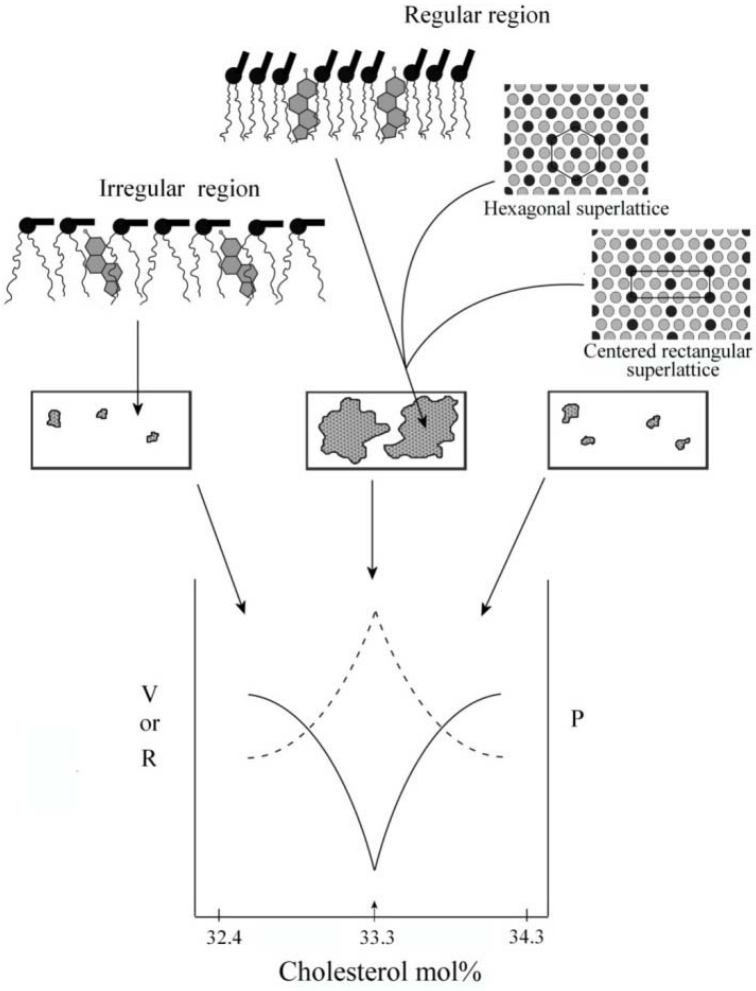

Figure 3. Schematic diagram showing the current concepts underlying the sterol regular distribution model.
The rectangle-like objects represent a lipid membrane, where regular (*shaded areas*) and irregular (*blank areas*) regions coexist. In regular regions, sterol molecules are regularly distributed into either hexagonal or centered rectangular superlattices within the host lipid matrix. There is a biphasic change in proportion of irregular region to regular region (*R, solid line*), membrane free volume (*V, solid line*), and the perimeter of regular region (*P, dashed line*) with membrane cholesterol content in the neighborhood of a critical sterol mole fraction C_r (e.g., 33.3 mol% cholesterol as indicated by arrow) theoretically predicted for maximal superlattice formation (taken from (Venegas, et al., 2007)).

CHAPTER 2

MATERIALS AND METHODS

2.1 Cell culture

The human MCF-7 breast cancer cells (from ATCC) were grown in Complete Growth Medium which included Dulbecco's Modification of Eagle's Medium (DMEM 1x, with 4.5g/L glucose, L-glucose & sodium pyruvate) supplemented with 10% Fetal Bovine Serum (FBS, BioWhittaker, Walkersville, MD) and 1% penicillin/streptomycin at 37°C with 5% CO_2 atmosphere until ~80% confluence. The cells were then detached with 0.25% trypsin and rinsed with phosphate-buffered saline (PBS), and collected after centrifugation at 2000 g for 5 min at 4^{o}C. Cells were resuspended into culture medium, plated into 96-well microplates and maintained in a serum-containing medium for 24 h until cells were attached to the wall of the wells in the microplates.

2.2 Preparation of liposomal CA4P

CA4P was obtained from Dr. Mohammad Kiani in the Mechanical Engineering Department. We first prepared CA4P-entrapped liposomes made of cholesterol and 1-palmitoyl-2-oleoyl-L-α-phosphatidylcholine (POPC). Calculated amounts of POPC and cholesterol in chloroform were pipetted into tubes and dried under N_2 until there was no visible solvent.

Lipids were then dried overnight under high vacuum. Next, lipids were reconstituted with 5.0 mL of 50 mM Tris-HCl buffer (pH 7.0) containing 30 mM CA4P, 0.02% NaN_3, and 0.1 mM EDTA at 37°C, then flushed with N_2 and vortexed for two minutes at 37°C to form multilamellar vesicles (MLVs). NaN_3 was used to prevent micro-organism growth in liposome dispersions. The MLVs were cooled to 4°C for 30 min and then incubated at 37°C for 30 min. This cooling-heating cycle was repeated three times to ensure an even distribution of lipids within each monolayer of the vesicles. After being exposed to three cycles of heating/cooling to allow for thorough mixing, vesicles were left for four days at room temperature to come to thermal equilibrium. During incubation, liposome samples were protected from light and heat, and were flushed with argon and sealed with Teflon-lined screw caps, in order to prevent auto-oxidation.

Four sample sets of cholesterol/POPC MLVs were prepared as described in Tables 3-6. They cover the following cholesterol mole fractions: 20.7-23.7 mol% (Table 3), 31.8-34.8 mol% (Table 4), 38.5-41.5 mol% (Table 5), and 48.5-51.5 mol% (Table 6). A typical sample set spanned a predicted critical sterol mole fraction for maximal superlattice formation. Every sample within the set contained the same absolute amount of cholesterol, but varied only in the cholesterol mole percent. This was accomplished by varying the number of moles of POPC per tube, while leaving the number of moles of sterols constant. Typically sterol mole percent was changed by 0.5 mol% for

each sample (Tables 3-6).

Large unilamellar vesicles (LUVs) were then prepared from MLVs by extrusion (Lipex Biomembranes Inc., Vancouver, BC, Canada). The MLVs were extruded at 37°C 10 times through two stacked 200-nm Nucleopore polycarbonate filters (Costar) under nitrogen gas pressure to form homogeneous LUVs. To avoid auto-oxidation of cholesterol, the LUV samples were then stored under N_2 at room temperature for ≥ 7 days prior to the cell proliferation assay.

Vesicle size was measured by photon correlation spectroscopy using the Malvern Zetasizer HS-1000 spectrometer (Malvern Worcs, UK; light source: 10 mW He-Ne laser at 633 nm). Size was determined before and immediately after extrusion (typically 100-150 nm in diameter). Our previous study (Wang, et al., 1998) showed that the sterol mole percents in vesicles before and after extrusion differ little (≤0.2 mol%). Thus, for convenience, the cholesterol mole percents in MLVs were used to assess the relationship between cholesterol content in liposomal CA4P and cell proliferation rate.

Immediately before the cell proliferation assay, free CA4P was removed by a Sephadex G-50 gel filtration column. The column was eluted with 50 mM Tris-HCl buffer (pH 7.0) containing 0.1 mM EDTA. The CA4P entrapped liposomes were then collected using a fraction collector (Biorad, Model 2110). Note that the elution buffer did not contain NaN_3. The level of NaN_3, which

was originally present in vesicles, became negligible in the pooled fractions and would not cause any cytotoxic effect on MCF-7 cells. The amount of CA4P in liposomes can be determined by first using extraction with choloform:methanol (2:1) plus an equal volume of Tris buffer (50 mM, pH 7.0). The entrapped CA4P (which is water soluble) was released from liposomes and partitioned into the aqueous phase. The absorbance at 340 nm of the aqueous phase was then measured on a Perkin-Elmer lambda-25 spectrophotometer in order to determine the amount of liposomal CA4P in the sample.

Table 3. Preparation of the cholesterol/POPC MLV sample set centered at C_r = 22.2 mol% cholesterol. Total volume = 2 mL.

Tube#	Chol mol%	[Total Lipid] mM	Total Lipid nmol	Chol nmol	POPC nmol
1	20.7	1.07	2144.9	444	1700.9
2	21.2	1.04	2094.3	444	1650.3
3	21.7	1.02	2046.1	444	1602.1
4	22.2	1.00	2000	444	1556
5	22.2	1.00	2000	444	1556
6	22.2	1.00	2000	444	1556
7	22.7	0.97	1955.9	444	1511.9
8	23.2	0.95	1913.7	444	1469.7
9	23.7	0.93	1873.4	444	1429.4

Table 4. Preparation of the cholesterol/POPC MLV sample set centered at C_r = 33.3 mol% cholesterol. Total volume = 2 mL.

Tube #	Chol mol%	[Total Lipid] mM	Total Lipid nmol	Chol nmol	POPC nmol
1	31.8	1.05	2094.3	666	1428.3
2	32.3	1.03	2061.9	666	1395.9
3	32.8	1.01	2030.5	666	1364.5
4	33.3	1.00	2000.0	666	1334
5	33.3	1.00	2000.0	666	1334
6	33.3	1.00	2000.0	666	1334
7	33.8	0.98	1970.4	666	1304.4
8	34.3	0.97	1941.7	666	1275.7
9	34.8	0.96	1913.8	666	1247.8

Table 5. Preparation of the cholesterol/POPC MLV sample set centered at C_r = 40.0 mol% cholesterol. Total volume = 2 mL.

Tube#	Chol mol%	[Total Lipid] mM	Total Lipid nmol	Chol nmol	POPC nmol
1	38.5	1.03	2077.9	800	1277.3
2	39.0	1.02	2051.3	800	1251.9
3	39.5	1.01	2025.0	800	1225.5
4	40.0	1.00	2000.0	800	1200.0
5	40.0	1.00	2000.0	800	1200.0
6	40.0	1.00	2000.0	800	1200.0
7	40.5	0.98	1975.9	800	1175.4
8	41.0	0.97	1951.7	800	1151.7
9	41.5	0.96	1927.4	800	1127.8

Table 6. Preparation of the cholesterol/POPC MLV sample set centered at C_r = 50.0 mol% cholesterol. Total volume = 2 mL.

Tube#	Chol mol%	[Total Lipid] mM	Total Lipid nmol	Chol nmol	POPC nmol
1	48.5	0.515	1030.9	500	530.9
2	49.0	0.510	1020.4	500	520.4
3	49.5	0.505	1010.1	500	510.1
4	50.0	0.500	1000.0	500	500.0
5	50.0	0.500	1000.0	500	500.0
6	50.0	0.500	1000.0	500	500.0
7	50.5	0.495	990.1	500	490.1
8	51.0	0.490	980.4	500	480.4
9	51.5	0.485	970.9	500	470.9

2.3 Cell proliferation assay

The extent of cancer cell proliferation was determined fluorometrically using a CyQUANT assay kit from Invitrogen-Molecular Probes. The operational procedures are described in Figure 4. The assay was done on MCF7 cells in the presence of varying cholesterol mole fractions in liposomal CA4P. The assay has a linear detection range extending from 50 or fewer to at least 500,000 cells in 2 mL volumes and is therefore ideal for cell proliferation studies as well as for routine cell counts.

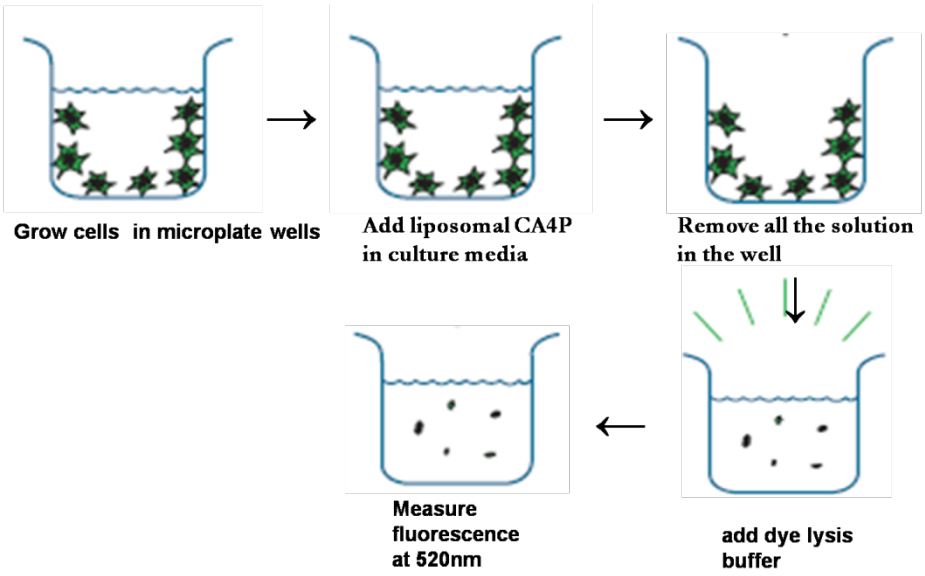

Figure 4. Operational procedures of the CyQUANT proliferation assay. The container represents one of the 96 wells in the microplate. Dead cells were removed with the solution from the well prior to adding dye lysis buffer. Only the alive cells that were attached to the wall of the well contributed to the fluorescence signals.

The assay is based on dye fluorescence enhancement upon binding to cellular nucleic acids. The resulting fluorescence intensity was measured at 530 nm on a Spectra Max M5 microplate reader (Molecular Devices,

Sunnyvale, CA) with excitation at 485 nm. The CyQUANT method is rapid and does not rely on cellular metabolic activity. Thus, cells can be frozen prior to assaying; time course assays are facile and data obtained from samples taken at widely different time intervals can be directly compared. We compare the cell proliferation rate of MCF-7 cells as a function of cholesterol content in liposomal drug formulations.

2.4 Statistical considerations

For the proliferation assay, six identical samples were used for each different liposomal CA4P formulation. Thus, the standard deviations of cell number can be obtained and used to evaluate if a biphasic change in cell number with cholesterol mole fraction is existent. A genuine peak or dip in the plot of cell number versus sterol mole fraction requires the peak height or the dip depth to be significantly greater than the standard deviations of the data. I did multiple Student's T-test for certain samples. For example, I have done Student's T test for the data in the sample set with 20.7-23.7 mol% cholesterol in Chol/POPC LUVs. The t value between sample at 22.2 mol% and sample at 20.7 mol% as cholesterol content is t_1=5.45; the t value between sample at 22.2mol% and sample at 21.7 mol% as cholesterol content is t_2=8.45; the t value between sample at 22.2mol% and sample at 22.7 mol% as cholesterol content is t_3=4.92; the t value between sample at 22.2mol% and sample at 23.2 mol% as cholesterol content is t_4=5.45. With

the degree of freedom df = 10, the critical value t_0 for P=0.005 is 3.16, $t_1 > t_0$, $t_2 > t_0$, $t_3 > t_0$, $t_4 > t_0$, so we can reject the null hypothesis and conclude that there is a significant difference between data at the sample with the C_r value 22.2mo% and the samples at the non-C_r values, with P<0.005.

The cholesterol mole fraction in liposomal formulation can be prepared to the accuracy of < 0.4% (Liu, et al., 1997, Wang, et al., 1998).

2.5 Summary of experimental design

The general experimental approaches of this thesis work are summarized in Figure 5. The first step was the preparation of CA4P entrapped POPC/cholesterol LUVs. Their sizes were about 150 nm in diameter with narrow size distributions (approximately ± 10 nm). Then free CA4P was removed by Sephadex G-50 column. The CA4P entrapped liposomes were collected using a fraction collector. Based on absorbance measurement at 340 nm (CA4P has maximum absorbance at this wavelength), the same amount of CA4P in the liposome form was pipette to each of the wells in the microplate, where ~10,000 MCF-7 cells/well were attached. After a given incubation time, the proliferation rate of the cells was measured.

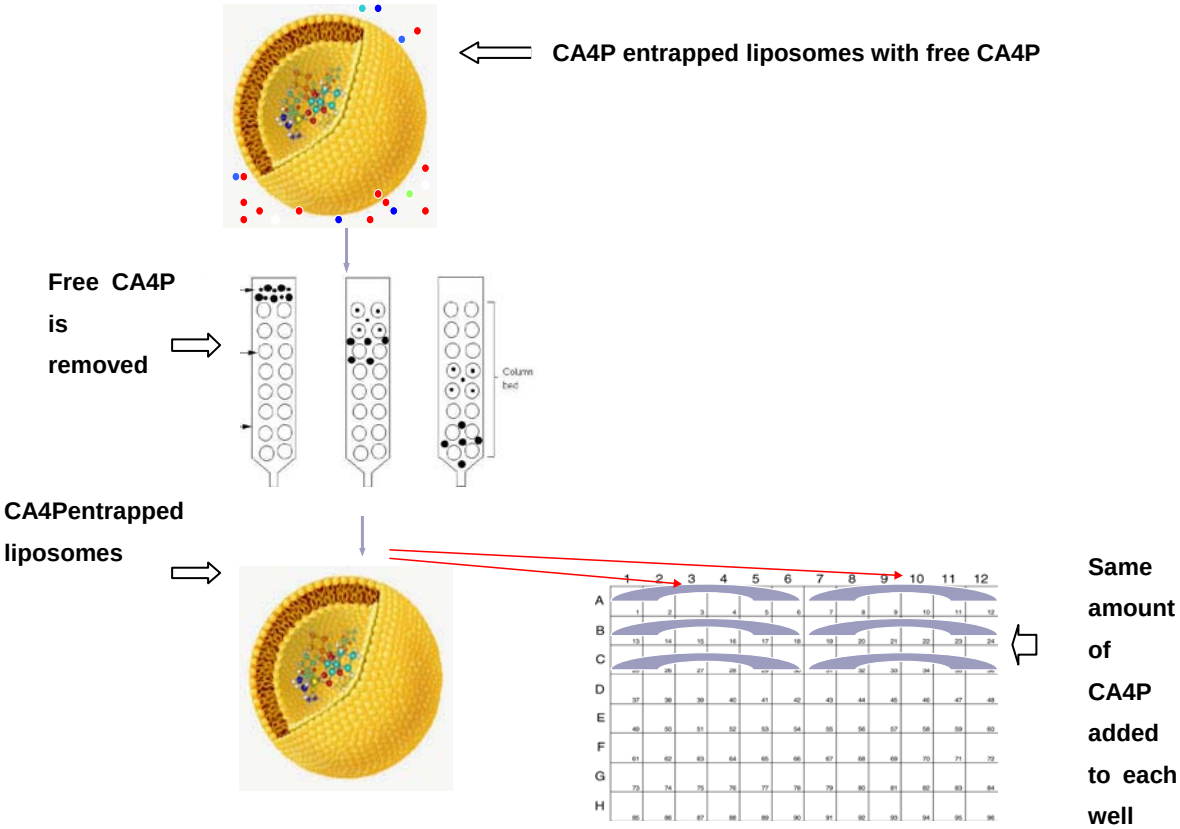

Figure 5. Schematic diagram showing the experimental design. The first step was the preparation of CA4P entrapped POPC/cholesterol LUVs. Then free CA4P was removed by Sephadex G-50 column. The CA4P entrapped liposomes were collected using a fraction collector. Based on absorbance measurement at 340 nm (CA4P has absorbance at this wavelength), the same amount of CA4P in the liposome form was pipetted into each of the wells in the microplate, where the cells were attached. After a given incubation time, we measured the proliferation rate of the cells.

CHAPTER 3

RESULTS

3.1 Separation of liposomal CA4P from free CA4P

Figure 6 shows that liposomes with entrapped CA4P can be separated from free CA4P. POPC/Chol liposomes with entrapped CA4P in a buffer containing free CA4P were loaded onto a Saphedex G-50 column (10.5 cm in length and 0.8 cm in diameter). Fractions of 9 drops were collected using a fraction collector. The scattered light from vesicles and the fluorescence intensity of CA4P were measured on an ISS K2 fluorometer. For the light scattering measurement, the excitation wavelength was set at 500 nm and the scatted light was detected at right angle through a monochromator set at 515 nm. The scattering intensity reflects the amount of lipid vesicles in the fractions. For the CA4P fluorescence intensity measurements, the excitation wavelength was set at 330 nm and the emission was observed at 400 nm. This is to measure both free CA4P and entrapped CA4P. Figure 6 (circles) shows that lipid vesicles came out in Fraction # 6, 7 and 8. In those fractions, the CA4P fluorescence intensity (sqaures) also exhibited a peak, due to the entrapped CA4P. The fluorescence intensity displayed a large peak starting from Fraction 15, which can be attributed to free CA4P. Fractions 6, 7, and 8 were pooled for the cell proliferation study.

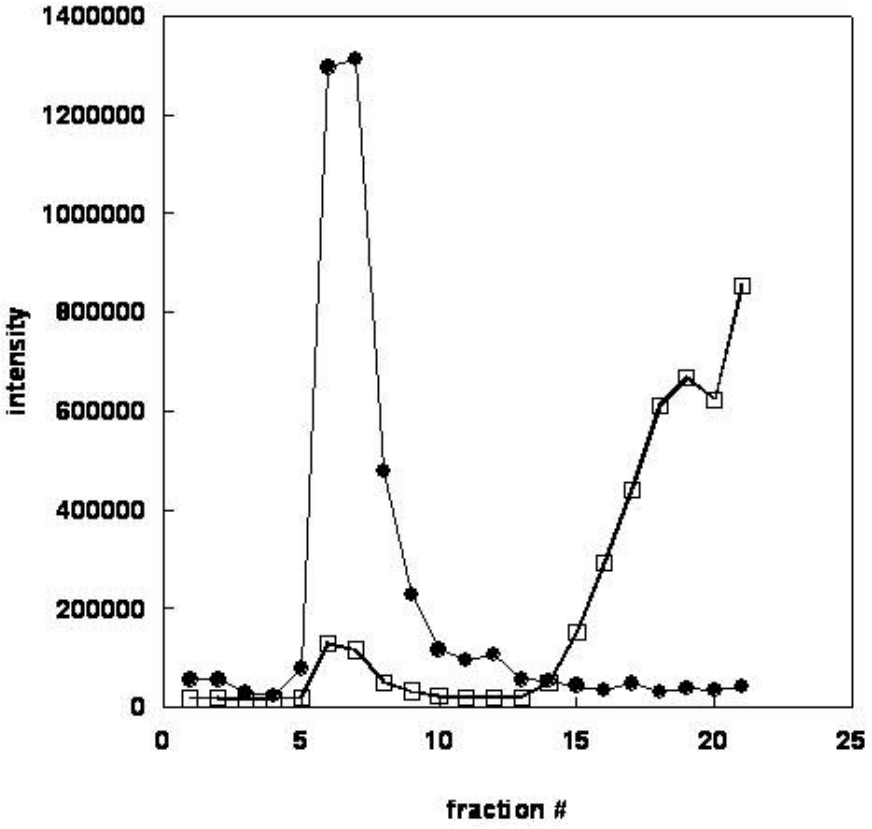

Figure 6. **Elution profile of POPC/cholesterol LUVs through a Sephadex G-50 column**

Each fraction contained 9 drops. Circles: light scatting intensities measured using $\lambda_{excitation}$= 500 nm and $\lambda_{emission}$ = 515 nm. Squares: fluorescence intensities measured using $\lambda_{excitation}$ = 330 nm and $\lambda_{emission}$ = 400 nm.

Using absorbance, we determined the relative amount of CA4P in liposomal CA4P collected from Sephadex G-50 gel filtration column. For this determination, 200 μL of the pooled liposomal CA4P was mixed with 2 mL chloroform:methanol (2:1, v/v) in a screw-caped test tube, followed by the addition of 2 mL buffer (~11 times dilution of the durg in the aqueous phase). The mixture was vortexed for 2 minutes. The upper layer (water layer) was taken out for absorbance measurement at 340 nm. This absorbance is a measure of the amount of CA4P entrapped in the liposomes.

For Abs_{340nm} in the cuvette = 0.005, $[CA4P]_{pooled}$ = (0.005/ε) x 11 x 1 cm = 9.75 x 10^{-6} M = 9.75 μM, where ε = 5640 $M^{-1}cm^{-1}$ is the extinction coefficient of CA4P in water at 340 nm (Venegas and Chong, unpublished results). Based on this calculation, we figured out the amount of liposomal CA4P needed to be pipetted out from the pooled fractions in order to deliver the same amount (in terms of nmole) of liposomal CA4P into each of the wells in the microplate for the cell proliferation assay. Typically, we added 0.5 nmole of CA4P (in the liposome form) to each of the wells in the microplate. In other words, in the cell proliferation assay, the number of cells (10,000 cells) and the amount of liposomal CA4P (0.5 nmole) in each well are the same. The only difference among the various samples within the same sample set was the cholesterol mole fraction in liposomal drug formulation.

3.2 Control experiments

Control experiments were carried out to determine the appropriate drug dose and the optimal incubation time between liposomal CA4P and MCF-7 cells for the cell proliferation assay.

3.2.1 Control Experiment 1. The experimental design of Control Experiment 1 is shown in Figure 7. The squares represent the wells in a 96-well microplate. To each well, 10000 cells were added. After an overnight incubation of cells in growth medium in the carbon dioxide incubator (37^{o}C), cells were almost fully attached to the wall of the wells. Then, the growth medium was pipetted out, and the cells became ready for the proliferation assay.

The time shown at the top of Figure 7 indicates the incubation time of liposomal CA4P with MCF-7 cells in the wells. Row A was for cells grown in the media in the absence of any liposomes or liposomal drugs. Row B contained cells plus 50 μL of 9.75 μM CA4P in liposomes composed of 30 mol% Chol and POPC (LUVs). Row C was for cells plus 50 μL of liposomes composed of POPC/Chol (30 mol%) in the absence of CA4P. Row H contained varying numbers of MCF-7 cells ranging from 500 to 10000 cells. The purpose of using Row H is to generate a standard curve correlating cell numbers to fluorescence intensities.

The standard curve is shown in Figure 8, where the fluorescence intensity varies almost linearly with cell number. The y-intercept does not go

to zero, which can be attributed to the background readings. Subtraction of the background is not needed because the standard curve is used for the purpose of comparison, not for determinations of the absolute values of the cell numbers.

Immediately after the CA4P entrapped liposomes were collected from the Sephadex G-50 column, 50 μL of 9.75 μM liposomal CA4P was added to each well at virtually the same time for the samples in the same sample set. In order to determine the optimal incubation time, the growth medium containing liposomal CA4P and dead cells (which were not attached to the wall) was pipetted out of the wells, one well at a time with 15 minute intervals (Figure 7). The number of cells remained attached to the wall was then determined by the proliferation assay as depicted in Figure 4. Specifically, at time = 15 min after the addition of liposomal CA4P, the solutions in A1 and B1 (Figure 7) were pipetted out. Similarly, at the time of 30 min (2X15 minutes), the solutions in A2 and B2 were taken out. In other words, at the time equal to n x 15 minutes, solutions in A_n and B_n were taken out. So the only difference among B1-B12 is the incubation time, as indicated in the top portion of Figure 7. Then, the observed difference in fluorescence signals between A_n and B_n can only be attributed to the effect of liposomal CA4P on MCF-7 cells.

The cell number as a function of incubation time is shown in Figure 9 for

MCF cells treated with liposomes alone (circles), treated with liposomal CA4P (squares), and not treated with liposomes or liposomal CA4P (triangles). The data (Figure 9) showed that liposomal CA4P induced a significant change in cell number over time (squares). The cell number decreased almost linearly with time until 90 min after addition of liposomal CA4P. The cell number reached a minimum at incubation time = ~150 min (squares, Figure 9). In contrast, liposomes alone (circles) did not induce any decrease in cell number, suggesting that the steady decrease in cell number over time shown in the squares (Figure 9) is due to the liposomal CA4P, not due to liposomes. Cells not treated with any liposomes (circles) and treated with liposomes alone (triangles) showed a slight increase in cell number over time, which is expected because cancer cells are supposed to proliferate over time in growth medium.

These data together indicate that the experimental conditions are appropriate for assessing the suppression effect of liposomal CA4P on the proliferation of MCF-7 cancer cells. The optimal incubation time for this proliferation assay under the current experimental conditions is about 90-150 minutes. The observation of a steady decrease in cell number over time upon addition of liposomal CA4P (squares, Figure 9) can be attributed to the anti-microtubule effect of the drug CA4P.

3.2.2 Control Experiment 2. Figure 10 shows that when the

liposomal CA4P dose was doubled from 0.5 nmole to 1.0 nmole, the profile of cell number versus incubation changed little. The optimal time was still ~150 min. This suggests that 50 μL of liposomal CA4P (Figures 7-9) would be sufficient for the proliferation assay.

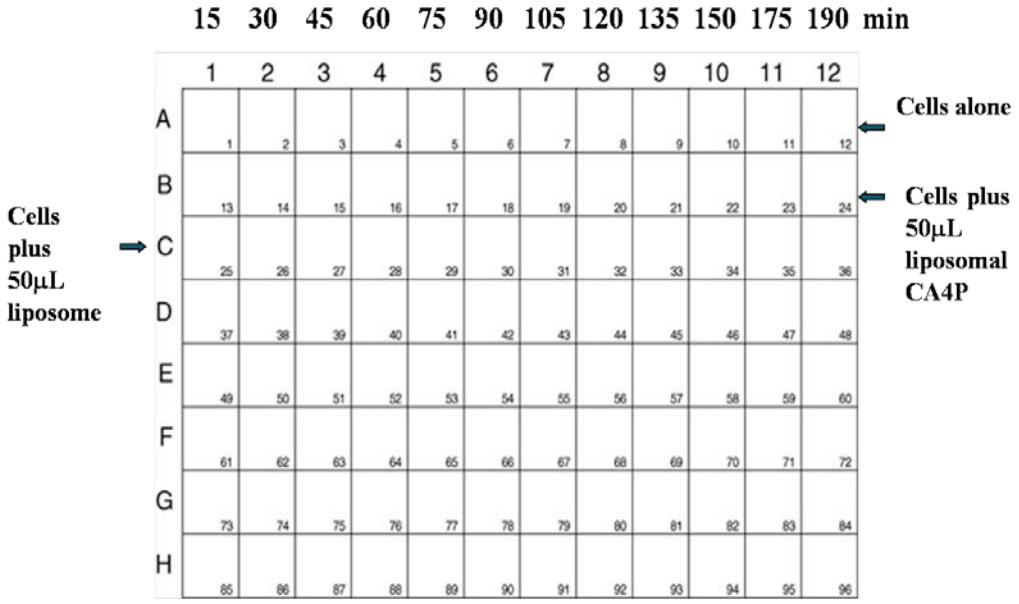

Figure 7. Design of Control Experiment 1

The squares represent the wells in a 96-well microplate. The incubation time of CA4P with MCF-7 cells in the wells is indicated at the top. Each well contained 10,000 cells at time zero. Row A: containing 10,000 MCF-7 cells in each well grown in the media but in the absence of any liposomes or liposomal drugs. Row B: containing 10,000 MCF-7 cells plus 50 μL of 11 μM Ca4P in liposomes composed of 30 mol% Chol and POPC (LUVs). Row C: containing 10,000 MCF-7 cells plus 50 μL of liposomes composed of POPC/Chol (30 mol%) in the absence of CA4P. Row H: containing varying numbers of MCF-7 cells ranging from 50 to 10000 cells in the absence of liposomes or liposomal drugs.

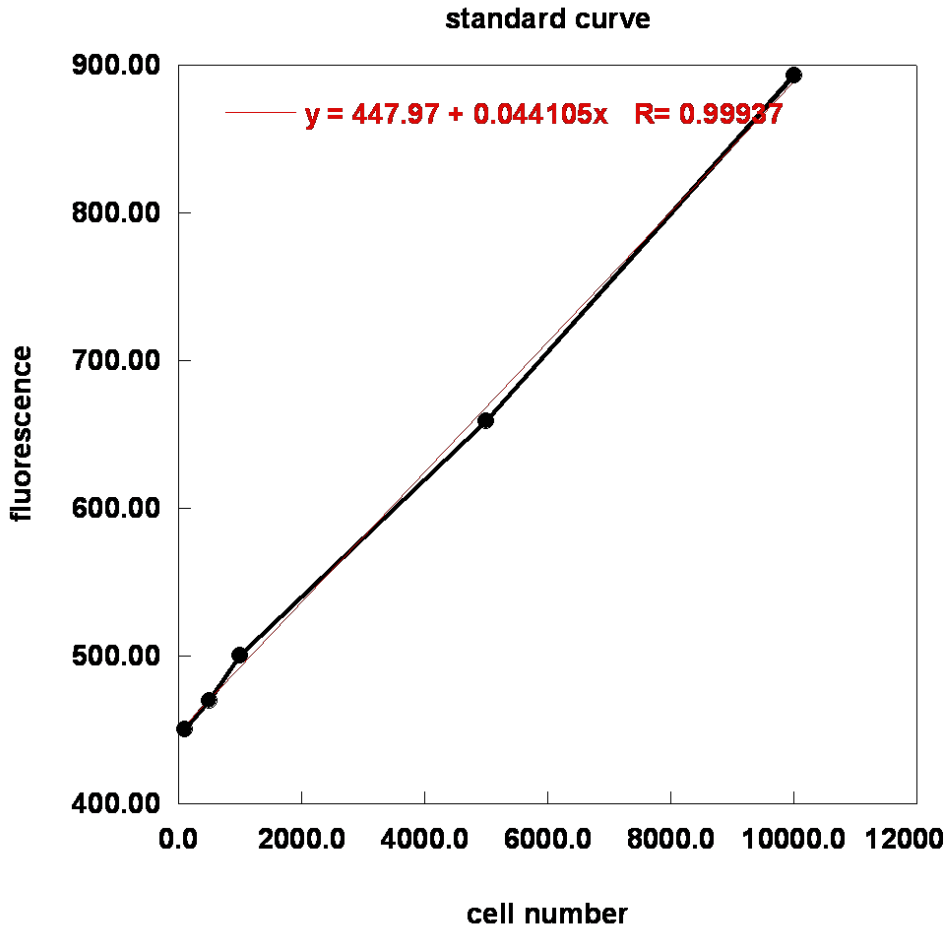

Figure 8. Standard curve of the CyQUANT cell proliferation assay for the control experiment

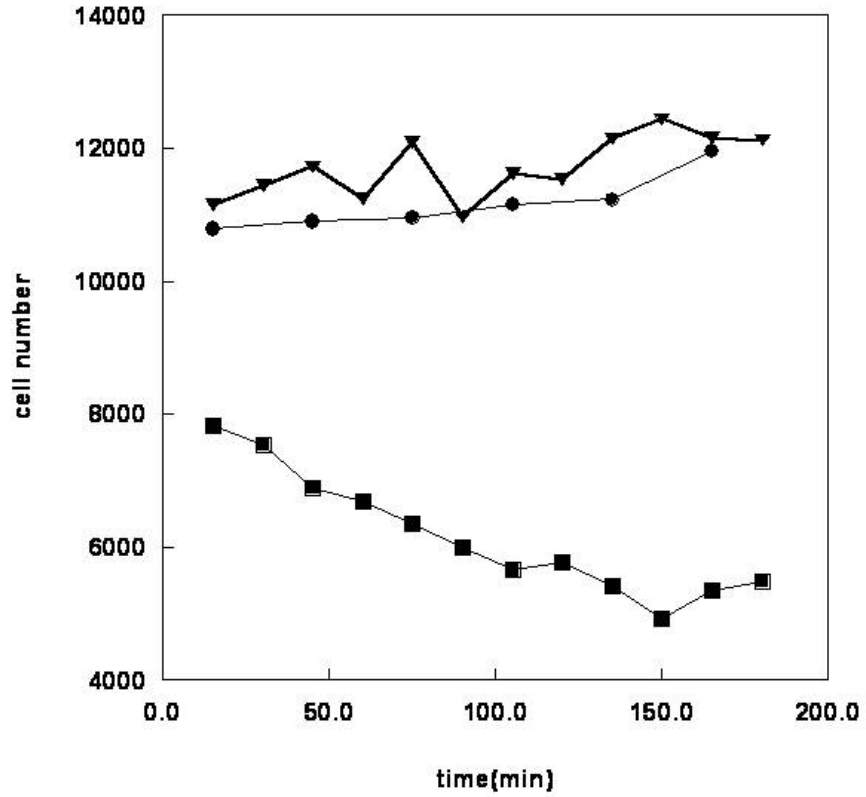

Figure 9. Effect of liposomes with and without drug on the proliferation of MCF-7 breast cancer cells

Circles: 50 μL of liposomes (30 mol% cholesterol in POPC) without CA4P was added to each well. Triangles: Each well contained MCF-7 cells alone without any liposomes or liposomal drugs or free drugs. Squares: 50 μL of 9.75 μM liposomal CA4P was added to each well. Each well contained 10,000 MCF-7 cells in growth medium (total volume of the sample in each well was 200 μL). Liposomes were composed of 30 mole% cholesterol and 70 mol% POPC.

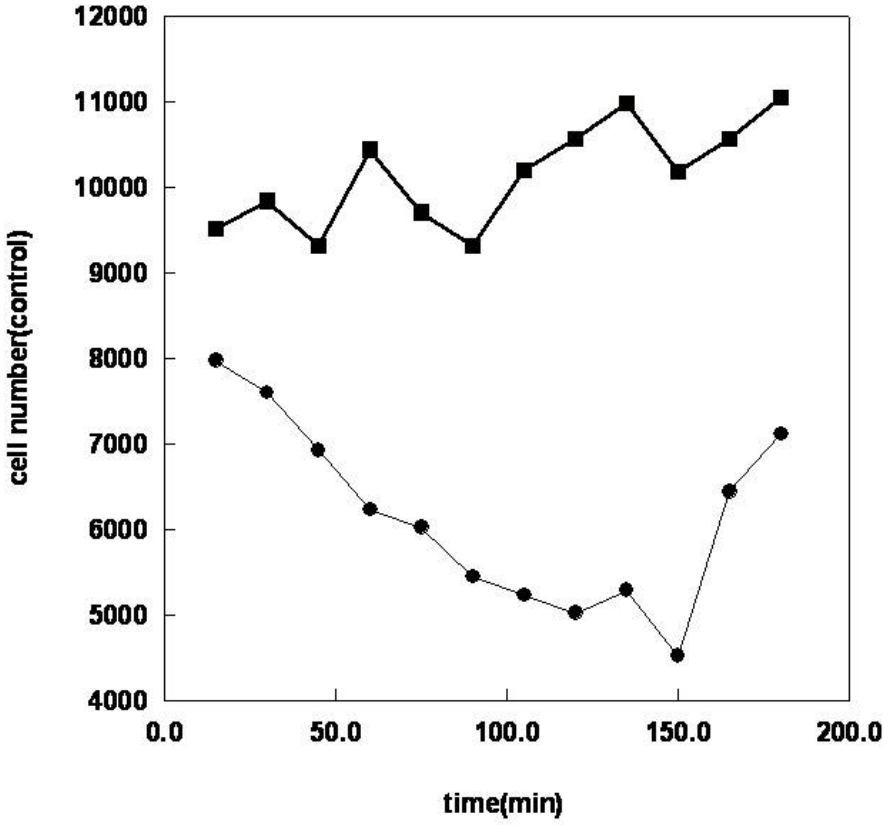

Figure 10. Time course of cell proliferation upon addition of two-times of liposomal CA4P to MCF7 cells

(Circles) 100 μL of 9.75 μM liposomal CA4P was added to each well which contained 10,000 cells in 100 μL growth medium at time zero. Liposomes were composed of 30 mol% cholesterol and 70 mol% POPC. Liposomal CA4P induced a steady decrease in cell number over time until ~150 min. (Squares) cells were not treated with any liposomes, showing only a slight increase in cell number over time.

3.3 Effects of cholesterol mole fraction in liposomal CA4P on MCF-7 cells

We prepared four sample sets to examine the effects of cholesterol mole fraction in liposomal CA4P on MCF-7 cell proliferation, as mentioned earlier. Figures 11, 12 and 13 show the results obtained from the sample set 20.7-23.7 mol% (Table 3). Figure 11 shows the raw data, that is, the fluorescence intensities recorded from the microplate reader for this sample set. Figure 12 shows the standard curve from the proliferation assay of this sample set. The error bars are the standard deviations from three independently prepared standard samples. A linear relationship was obtained between the cell number and the fluorescence intensity. Based on the standard curve, we converted the fluorescence intensities measured to the cell numbers in the wells. Figure 13 shows the effect of liposomal cholesterol content on the cell numbers in the wells after the samples being treated with the liposomal CA4P for 90 min (see Materials and Methods). The vertical bars in Figure 13 are the standard deviations from six independently treated samples. It is clear from Figure 13 that the cell proliferation rate (cell number change per 90 min) varies with the cholesterol mole fraction in liposomal formulation in a biphasic manner showing a minimum in cell number at 22.2 mol%. This cholesterol mole fraction (22.2 mol% cholesterol) is one of the theoretically predicted sterol mole fractions for maximum sterol superlattice formation.

	1	2	3	4	5	6	7	8	9	10	11	12
A	382.02	383.01	340.53	384.02	389.62	379.01	360.82	366.21	360.24	358.03	356.80	361.92
B	315.90	310.02	305.24	313.29	318.63	312.04	300.75	304.29	298.36	301.24	306.94	298.37
C	387.71	395.48	386.83	389.80	390.92	392.97	412.98	418.24	406.89	409.08	412.52	409.01
D												
E	174.22	202.08	236.06	350.42	550.28							
F	183.05	198.10	243.42	359.10	556.06							
G	182.95	197.08	242.64	348.35	548.45							
H												

Figure 11. The fluorescence intensities measured on a microplate reader for the sample set 20.7-23.7 mol% cholesterol in Chol/POPC LUVs

The squares represent the 96 wells in the microplate. A1-A6 for 20.8 mol% cholesterol (6 repeats in order to obtain the average and standard deviations); A7-12 for 21.8 mol%; B1-6 for 22.2 mol%; B7-12 for 22.2 mol% (a repeat); C1-6 for 22.8 mol%; C7-12 for 23.2 mol%; E1-5 for stardards of 500, 1000, 2000, 5000, and 10000 MCF-7 cells, respectively; F1-5 and G1-5 are the repeats of E1-5 in order to obtain standard deviations for the data points in the standard curve.

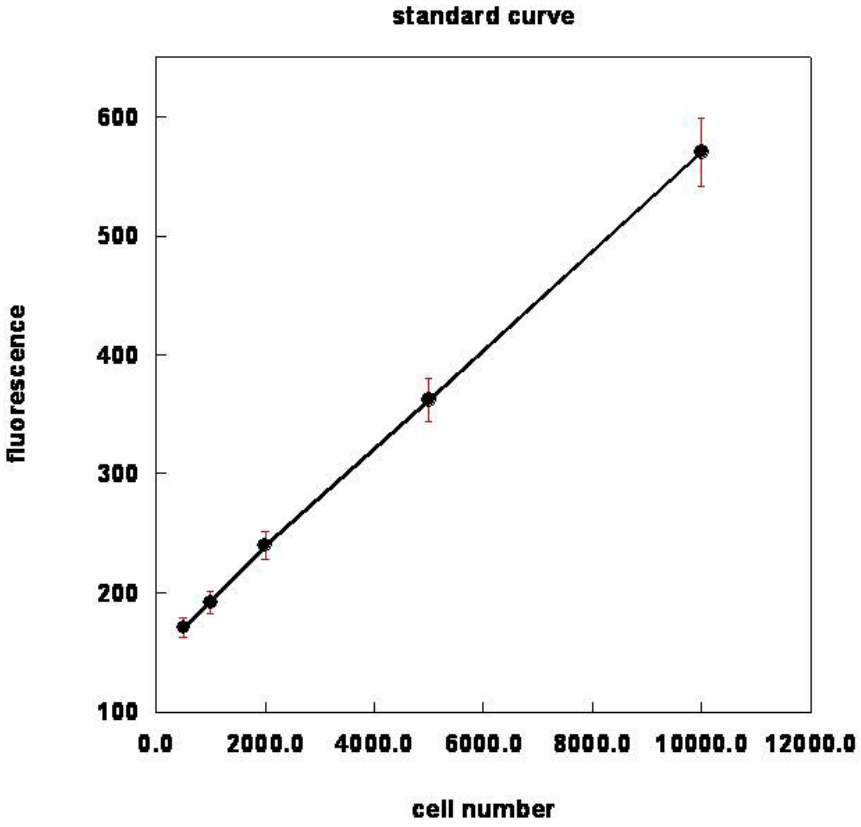

Figure 12. Standard curve of the cell proliferation assay for the sample set 20.7-23.7 mol% cholesterol in Chol/POPC LUVs

The raw data are shown in Figure 11.

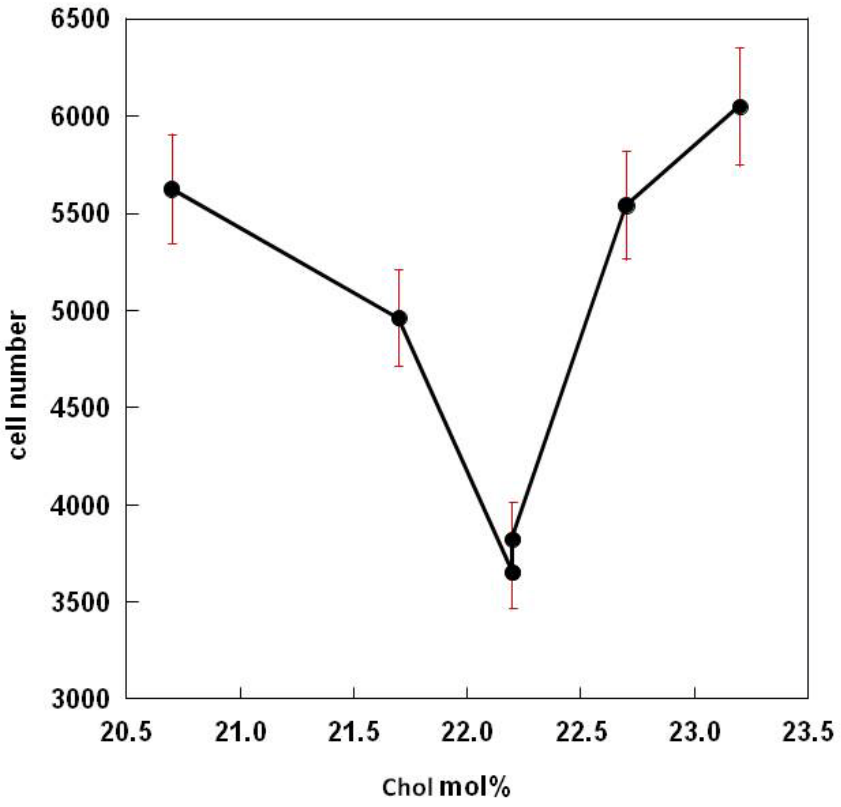

Figure 13. Effect of liposomal cholesterol mole fraction on cell number after 90 min incubation of MCF-7 breast cancer cells with liposomal CA4P

The amount of CA4P introduced to each well (containing 10,000 cells at time zero) was ~0.5 nmole. The vertical bars are the standard deviations of the cell numbers from six independently treated samples.

The data obtained from the sample set 31.8-34.8 mol% (Table 4) are shown in Figures 14, 15, and 16 for Experiment 1 and in Figures 17, 18, and 19 for Experiment 2. In this sample set, 33.3 mol% cholesterol is the only critical sterol mole fraction for maximal sterol superlattice formation. Both Experiment 1 and Experiment 2 showed that, after 90 min incubation with liposomal CA4P, the number of MCF7 cells decreased most when using liposomal drug formulation at 33.3 mol% cholesterol (Figures 16 and 19). We did this experiment twice to confirm the conclusion that there is a biphasic change in cell number at 33.3 mol% cholesterol. These data show again that the tubulin-disrupting effect is most prominent at the critical sterol mole fraction for maximal superlattice formation than at the nearby non-critical mole fractions.

	1	2	3	4	5	6	7	8	9	10	11	12
A	446.02	449.01	450.53	448.02	451.62	448.01	421.82	426.21	429.24	428.03	424.80	431.92
B	445.90	450.02	448.24	443.29	448.63	442.04	410.75	404.29	408.36	411.24	406.94	408.37
C	397.71	395.48	401.83	409.80	300.92	392.97	422.98	428.24	416.89	429.08	422.52	421.01
D	468.40	454.94	460.84	457.05	459.25	461.25						
E	182.03	206.17	249.49	360.15	549.55							
F												
G												
H												

Figure 14. The fluorescence intensities measured on a microplate reader for the sample set 31.8-34.8 mol% cholesterol in Chol/POPC LUVs (Experiment 1)

The squares represent the 96 wells in the microplate. A1-A6 for 31.8 mol% (6 repeats in order to obtain the average and standard deviations); A7-12 for 32.3 mol%; B1-6 for 32.8 mol%; B7-12 for 33.3 mol%; C1-6 for 33.3 mol%; C7-12 for 34.3 mol%; D1-6 for 34.8 mol%. E1-5 for stardards of 500, 1000, 2000, 5000, and 10000 MCF-7 cells, respectively.

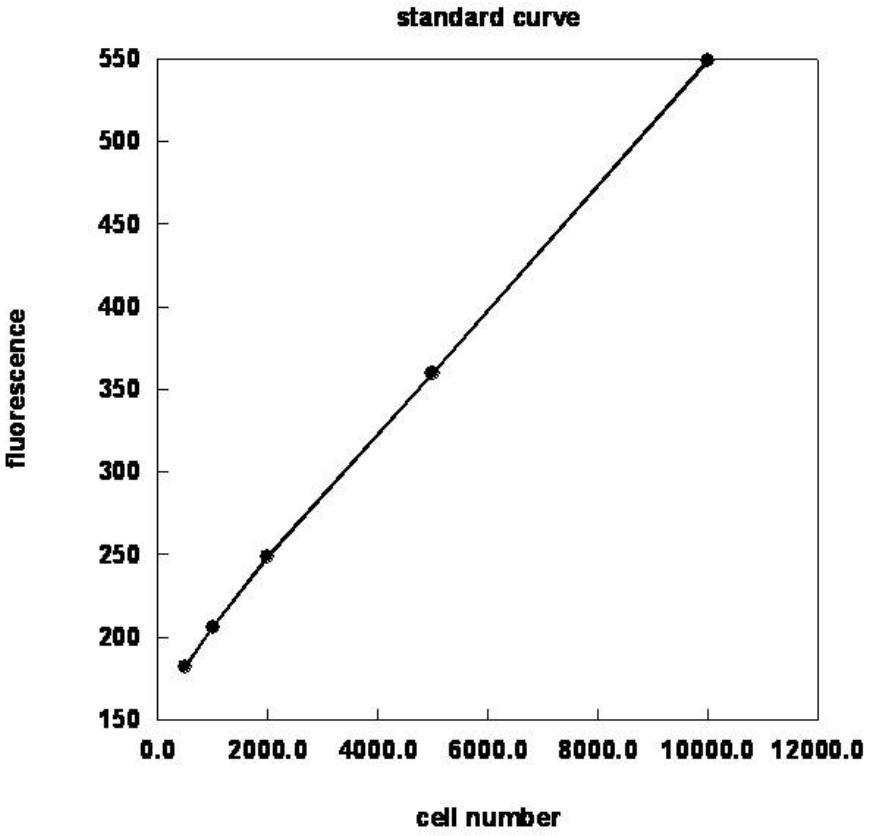

Figure 15. Standard curve of the cell proliferation assay for the sample set 31.8-34.8 mol% cholesterol in Chol/POPC LUVs (Experiment 1).

The raw data are shown in Figure 14.

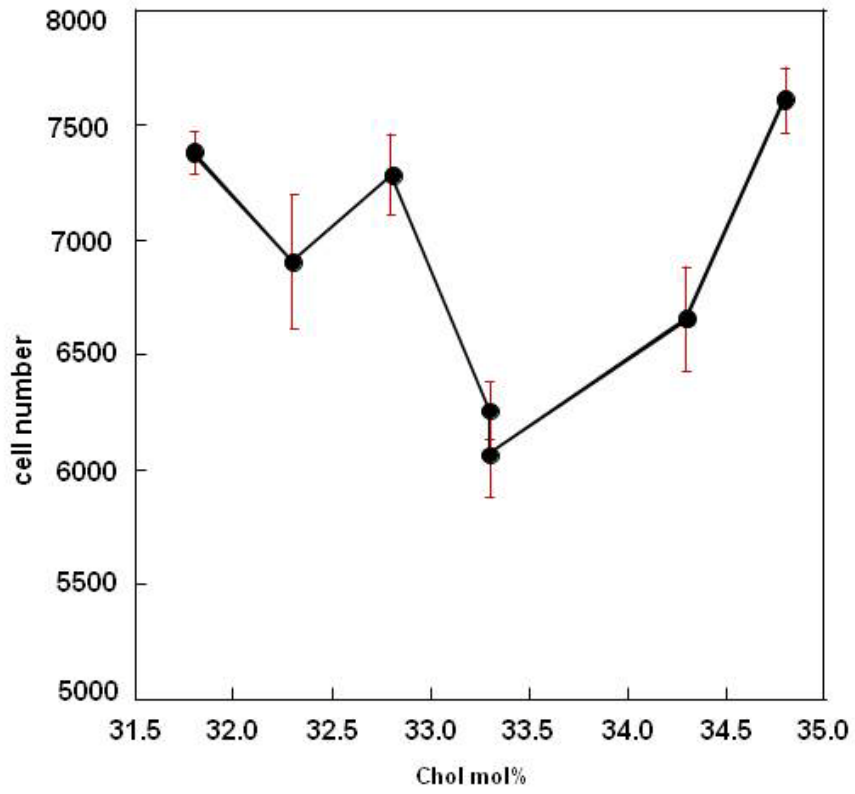

Figure 16. Effect of cholesterol mole fraction, in the range of 31.8-34.8 mol%, in Chol/POPC LUVs on cell numbers after 90 min incubation of MCF-7 breast cancer cells with liposomal CA4P (Experiment 1)

The amount of CA4P introduced to each well (containing 10,000 cells at time zero) was ~0.5 nmole. The vertical bars are the standard deviations of the cell numbers from six independently treated samples.

	1	2	3	4	5	6	7	8	9	10	11	12
A	442.02	449.01	440.53	438.02	441.62	444.01	421.82	426.21	420.24	428.03	426.80	431.92
B	395.90	400.02	395.24	393.29	398.63	392.04	390.75	394.29	398.36	391.24	386.94	388.37
C	417.71	405.48	406.83	409.80	410.92	412.97	432.98	438.24	446.89	439.08	442.52	435.01
D												
E												
F												
G												
H	158.23	190.27	237.41	344.35	532.45							

Figure 17. The fluorescence intensities measured on a microplate reader for the sample set 31.8-34.8 mol% cholesterol in Chol/POPC LUVs (Experiment 2)

This is a repeat of the experiment shown in Figures 14-16. The fluorescence intensities measured on a microplate reader for the sample set 31.8-34.8 mol% cholesterol in Chol/POPC LUVs. A1-A6 for 31.8 mol% (6 repeats in order to obtain the average and standard deviations); A7-12 for 32.8 mol%; B1-6 for 33.3 mol%; B7-12 for 33.3 mol%; C1-6 for 34.2 mol%; C7-12 for 34.8 mol%. E1-5 for stardards of 500, 1000, 2000, 5000, and 10000 MCF-7 cells, respectively.

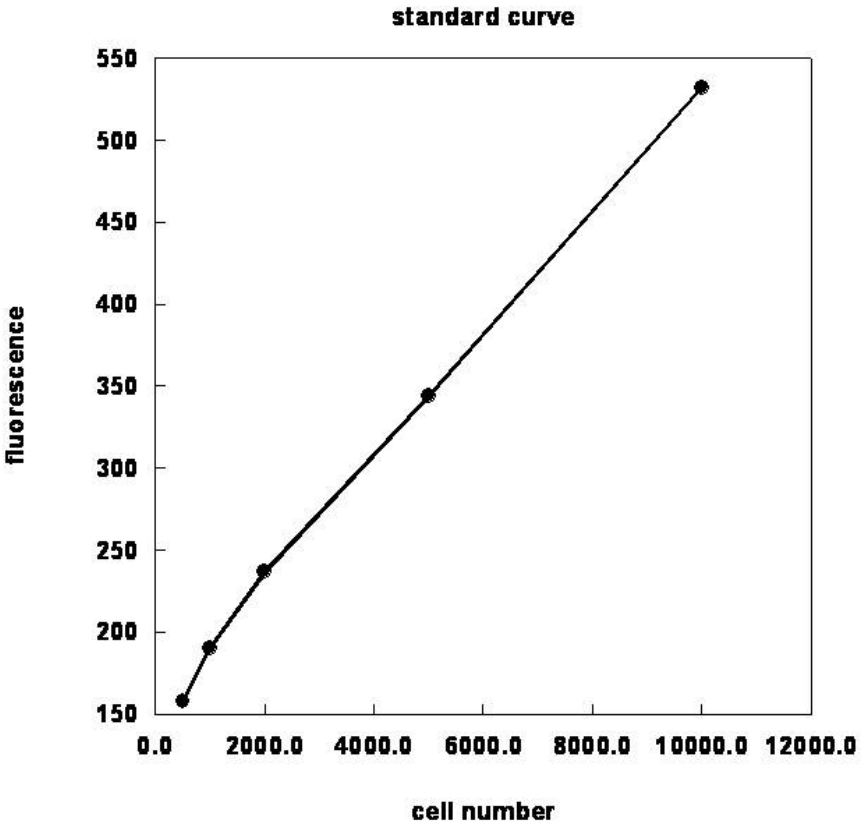

Figure 18. Standard curve of the cell proliferation assay for the sample set 31.8-34.8 mol% cholesterol in Chol/POPC LUVs (Experiment 2)

The raw data are shown in Figure 17.

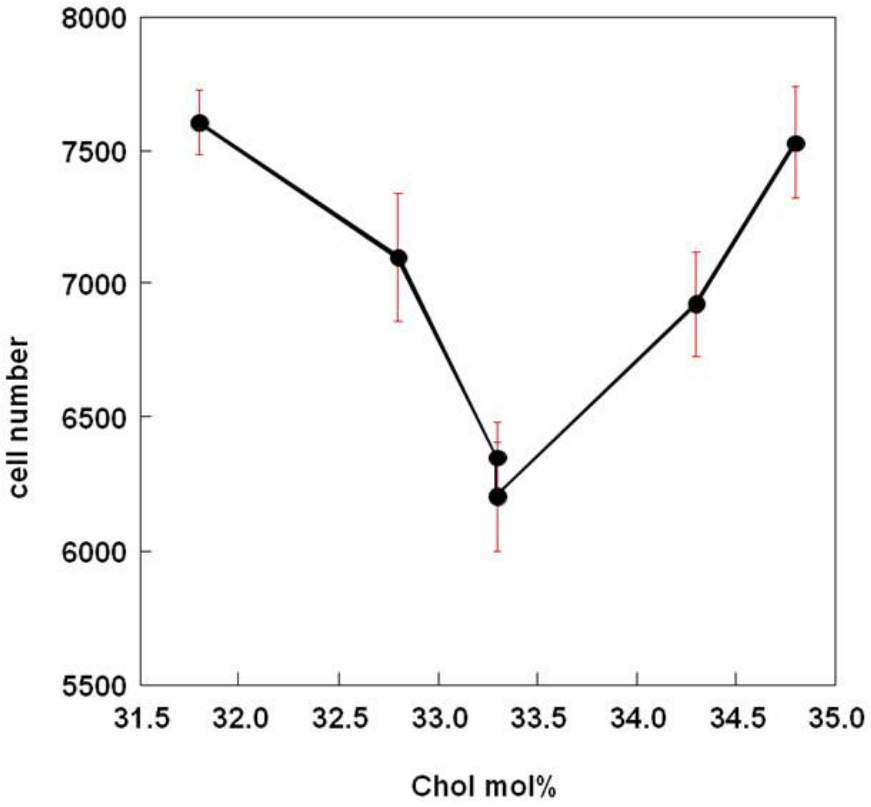

Figure 19. Effect of cholesterol mole fraction, in the range of 31.8-34.8 mol%, in Chol/POPC LUVs on cell numbers after 90 min incubation of MCF-7 breast cancer cells with liposomal CA4P (Experiment 2)
This is a repeat of the experiment described in Figures 14-16. The amount of CA4P introduced to each well (containing 10,000 cells at time zero) was ~0.5 nmole. The vertical bars are the standard deviations of the cell numbers from six independently treated samples.

The data for the sample set 38.5-41.5 mol% (Table 5) are given in Figures 20, 21, and 22. The only critical sterol mole fraction in this sample set is 40.0 mol%. It is clear from Figure 22 that there is a biphasic change in cell proliferation at 40.0 mol%.

The data for the sample set 48.5-51.5 mol% (Table 5) are given in Figures 23, 24, and 25. Here the only critical sterol mole fraction is 50.0 mol% cholesterol. The data in Figure 25 show an alternating variation of cell proliferation with cholesterol mole fraction, displaying a minimum at 50.0 mol%.

	1	2	3	4	5	6	7	8	9	10	11	12
A	452.52	463.09	450.23	454.92	459.62	499.01	430.82	426.21	420.24	428.03	426.89	418.02
B	435.90	440.42	425.24	433.25	438.63	442.44	420.75	424.29	428.36	421.24	416.94	418.37
C	417.71	415.48	406.23	409.89	410.92	419.77	392.98	390.24	406.89	399.01	402.52	399.01
D	442.82	444.08	442.06	438.45	439.08	438.82	477.83	479.84	480.67	482.62	483.68	472.71
E	182.22	204.08	246.06	350.42	550.28							
F	183.05	198.10	247.42	349.10	562.06							
G	179.95	190.08	242.64	358.35	568.45							
H												

Figure 20. The fluorescence intensities measured on a microplate reader for the sample set 38.5-41.0 mol% cholesterol in Chol/POPC LUVs

The squares represent the 96 wells in the microplate. A1-A6 for 38.6 mol% (6 repeats in order to obtain the average and standard deviations); A7-12 for 39.0 mol%; B1-6 for 39.5 mol%; B7-12 for 40.0 mol%; C1-6 for 40.0 mol%; C7-12 for 40.0 mol%; D1-6 for 40.5 mol%; D7-12 for 41.0 mol%. E1-5 for stardards of 500, 1000, 2000, 5000, and 10000 MCF-7 cells, respectively; F1-5 and G1-5 are the repeats of E1-5 in order to obtain standard deviations for the data points in the standard curve.

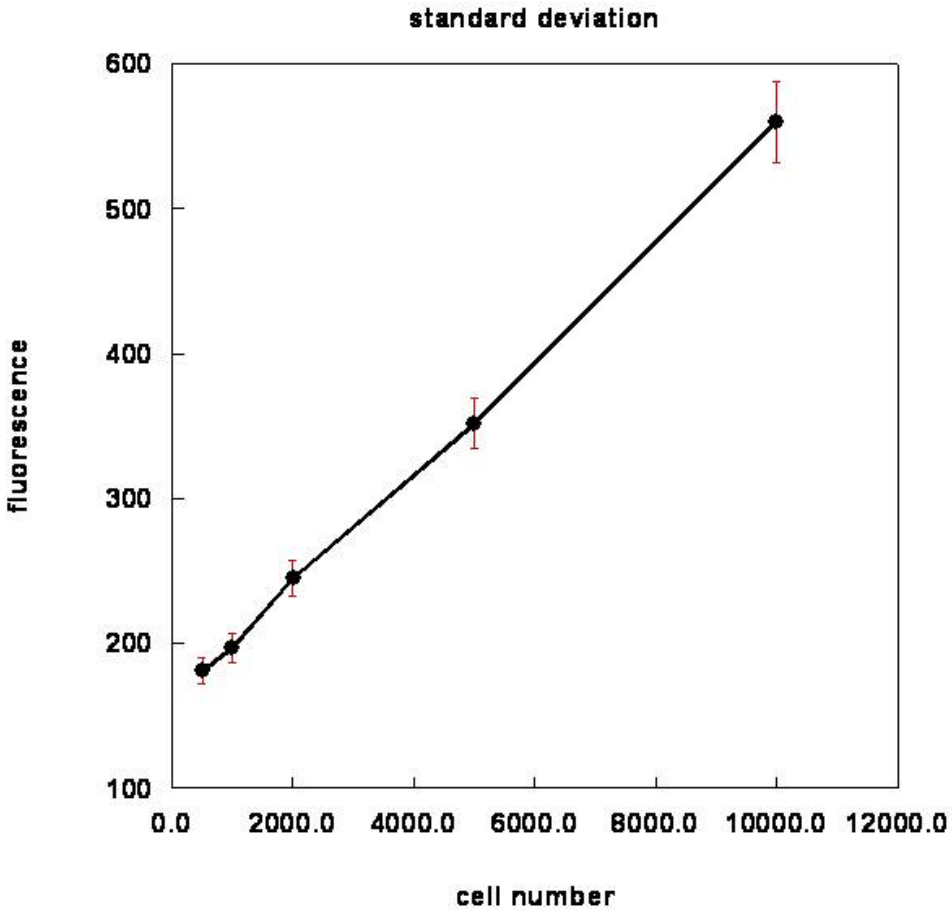

Figure 21. Standard curve of the cell proliferation assay for the sample set 38.5-41.0 mol% cholesterol in Chol/POPC LUVs
The raw data are shown in Figure 20.

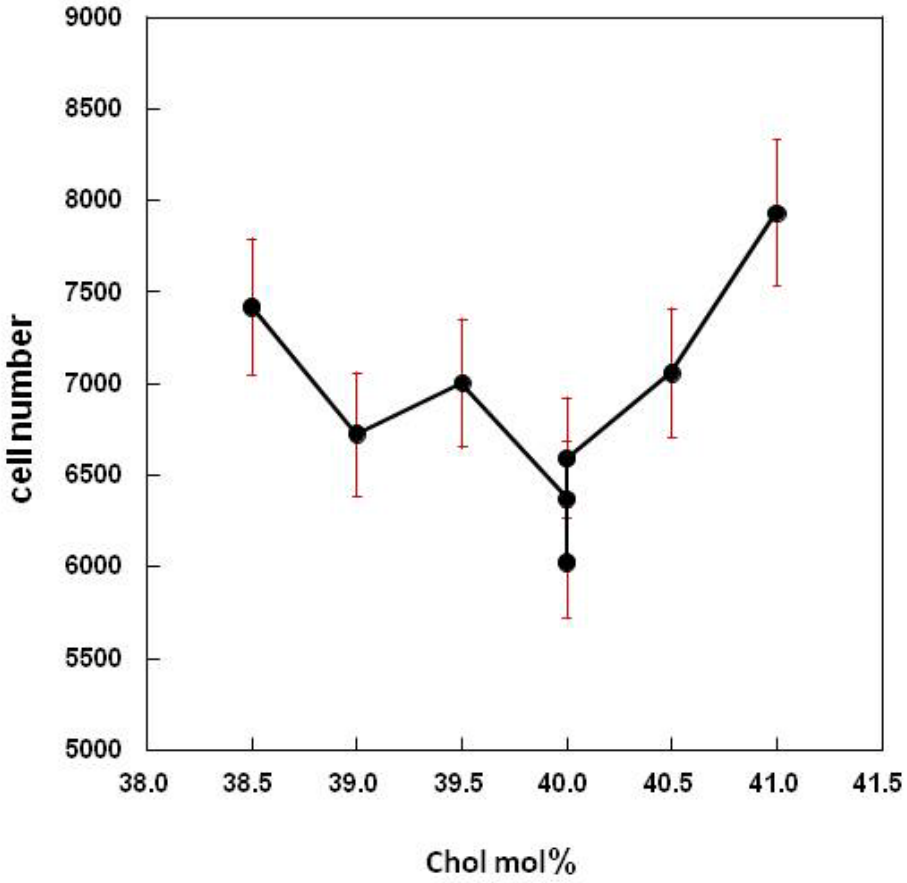

Figure 22. Effect of cholesterol mole fraction, in the range of 38.5-41.5 mol%, in Chol/POPC LUVs on cell numbers after 90 min incubation of MCF-7 breast cancer cells with liposomal CA4P

The amount of CA4P introduced to each well (containing 10,000 cells at time zero) was ~0.5 nmole. The vertical bars are the standard deviations of the cell numbers from six independently treated samples.

	1	2	3	4	5	6	7	8	9	10	11	12
A	492.52	483.09	490.23	484.92	489.62	499.01	470.82	476.21	460.24	472.03	466.89	469.02
B	405.90	410.42	405.24	413.25	415.63	402.44	390.25	381.20	398.66	381.24	386.94	378.37
C	427.71	415.48	420.23	429.89	420.92	429.77	445.26	439.35	442.68	432.35	440.36	443.45
D												
E	172.22	194.08	236.06	350.42	550.28							
F	169.95	190.08	242.64	358.35	558.45							
G	173.05	193.10	240.42	345.10	542.06							
H												

Figure 23. The fluorescence intensities measured on a microplate reader for the sample set 48.5-51.5 mol% cholesterol in Chol/POPC LUVs

The squares represent the 96 wells in the microplate. A1-A6 for 48.5 mol% (6 repeats in order to obtain the average and standard deviations); A7-12 for 49.5 mol%; B1-6 for 50.0 mol%; B7-12 for 50.0 mol%; C1-6 for 50.5 mol%; C7-12 for 51.0 mol%; E1-5 for stardards of 500, 1000, 2000, 5000, and 10000 MCF-7 cells, respectively; F1-5 and G1-5 are the repeats of E1-5 in order to obtain standard deviations for the data points in the standard curve.

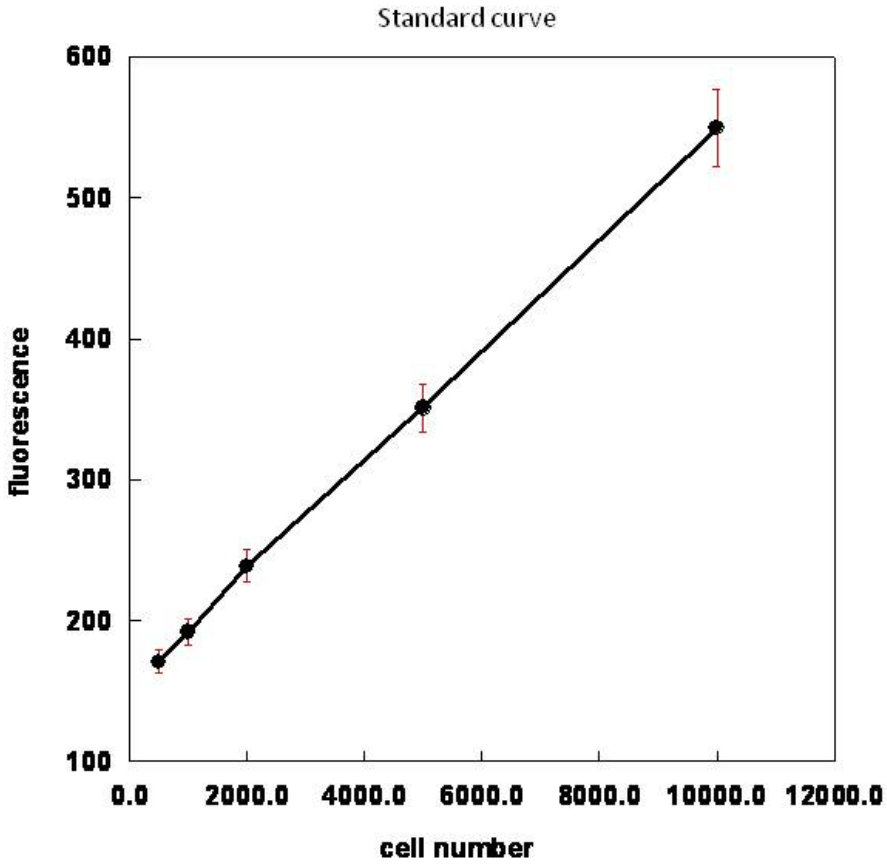

Figure 24. Standard curve of the cell proliferation assay for the sample set 48.5-51.5 mol% cholesterol in Chol/POPC LUVs
The raw data are shown in Figure 23.

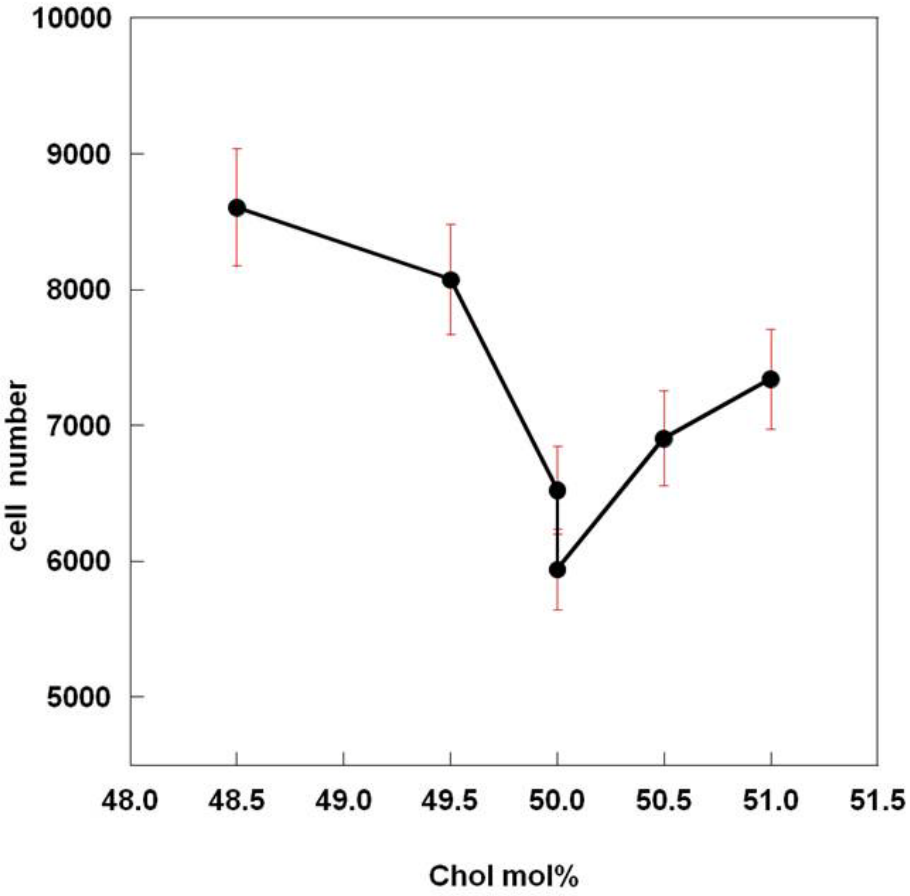

Figure 25. Effect of cholesterol mole fraction, in the range of 48.5-51.5 mol%, in Chol/POPC LUVs on cell numbers after 90 min incubation of MCF-7 breast cancer cells with liposomal CA4P
The amount of CA4P introduced to each well (containing 10,000 cells at time zero) was ~0.5 nmole. The vertical bars are the standard deviations of the cell numbers from six independently treated samples.

CHAPTER 4

GENERAL DISCUSSION AND CONCLUSIONS

4.1 How to interpret the biphasic change of cell proliferation with liposomal cholesterol content

In this thesis work, I examined how cholesterol mole fraction in liposomal formulations affects the anti-proliferation activity of CA4P. Four sets of liposome samples have been tested. They cover four different cholesterol mole fraction regions, namely, 20.7-23.7 mol%, 31.8-34.8 mol%, 38.5-41.5 mol%, and 48.5-51.5 mol%. Each region covers only one critical sterol mole fraction (C_r) theoretically predicted for maximal sterol superlattice formation. These C_r values are 22.2, 33.3, 40.0 and 50.0 mol% (Chong and Olsher, 2004, Chong, et al., 2009). In each of the samples for the proliferation assay, the cell number at time zero was fixed to 10,000 and the amount of liposomal CA4P added was fixed to ~0.5 nmole. According to the conventional biochemistry knowledge, one would predict the same cell proliferation rate for all the samples examined. However, our data show that this is not the case. Instead, we demonstrate that the cell proliferation rate varies with liposomal drug cholesterol content in a biphasic manner, reaching a local minimum at those C_r values. These results are novel and can be interpreted only by the sterol superlattice model.

According to the theory of sterol superlattice, the perimeter of the

regularly distributed sterol superlattice domains reaches a local maximum at C_r (Figure 3). The perimeter region is referred to as the interfacial region between regular and irregular distributions. Through the rather disordered interfacial region, CA4P should be released from the liposomes more easily. It is then logical to propose that when the interfacial region reaches a local maximum at C_r (such as 33.3 mol%), more CA4P molecules are released and they are released at a faster rate. As a result, more MCF-7 cells are disrupted and fewer cells are proliferated.

To the best of our knowledge, our present data can only be interpreted by the sterol superlattice model. In fact, in a separate study by Dr. Venegas in our laboratory, it is found that the release rate of CA4P from cholesterol/POPC LUVs reaches a local maximum at C_r (Venegas and Chong, unpublished data), which fully supports our data interpretation.

4.2 Significance

This work is significant from a biophysical point of view because it provides additional supporting evidence for the sterol superlattice model. Cholesterol lateral organization in the membrane is a long standing problem, which is of fundamental importance in understanding the role of cholesterol in membranes or cells. Because there is no technology allowing us to directly visualize the lateral organization of lipid molecules in the fluid membrane at the molecular resolution, the sterol superlattice model has not been

universally accepted yet. However, many pieces of spectroscopic and functional evidence supporting this model have been reported in the literature. For example, we have previously demonstrated that the activities of membrane surface acting enzymes such as phospholipase A2 (Liu and Chong, 1999) and cholesterol oxidase (Wang, et al., 2004), the rate of free radical-induced sterol oxidation (Olsher, et al., 2005, Olsher and Chong, 2008) and the partitioning of the antifungal drug nystatin into membranes (Wang, et al., 1998) are all regulated by the extent of sterol superlattice in the membrane. Here we show that the activity of liposomal CA4P against breast cancer cell proliferation is also regulated by the extent of sterol superlattice showing a maximal activity at the critical sterol mole fractions for maximal superlattice formation. The present results are in full agreement with the sterol superlattice model, thus providing another piece of functional evidence for the formation of sterol superlattices in cholesterol-containing membranes.

This work is also highly significant from a biopharmaceuticals point of view. As mentioned earlier, 75% of current anticancer liposomal drug formulations include cholesterol as a major component. The purpose was to stabilize the liposomes. Here we demonstrate that cholesterol is not just serving as a stabilizing agent. Actually cholesterol content can modulate the activity of liposomal drugs. Hence, one may use the concept of sterol superlattice formation to optimize the design of liposomal drugs in general

and liposomal CA4P in particular. This provides a rational design and avoids empirical testing, which is time consuming.

4.3 Future works

This thesis work is to use Chol/POPC liposomal CA4P and MCF-7 cancer cells to demonstrate a new physical principle governing the interactions of liposomal drugs with cells. This physical principle should be applicable to many different liposome systems, different anticancer drugs, and different cancer cells.

It is also of interest to investigate whether the extent of sterol superlattice in liposomal drugs affects the mechanisms of drug uptake by cells, either by endocytosis or by membrane fusion.

Although our present data show a minimal cancer cell proliferation rate for cells treated with liposomal CA4P at critical sterol mole fractions (C_r) for maximal superlattice formation, we cannot claim at the present time that liposomal CA4P at C_r is the best formulation for treating cancers. Obviously we need to extend the study to animal models. If the time for liposomes to reach the target, i.e., tumors, is much shorter than the time for spontaneous drug release in the circulation, then there is a high possibility that liposomal CA4P is most effective in suppressing cancer cell growth when the liposomal cholesterol content is at C_r. On the other hand, if the time to reach the target

is much longer than the time for spontaneous drug release, then there is a high possibility that liposomal CA4P is least effective when the liposome cholesterol content is at C_r. In any case, our present study provides a start point to think about using the concept of sterol superlattice in designing liposomal anticancer drugs. This strategy, when used in combination with radiation therapy and targeted delivery, should significantly increase the overall therapeutic efficacy of the liposomal anticancer drugs.

4.4 Conclusions

In conclusion, we have demonstrated here that the anti-cancer activity (e.g., cell growth suppression) of liposomal CA4P varies with the cholesterol mole fraction in the liposomal formulation in a biphasic manner, displaying a local maximum at C_r. This result can only be interpreted by the sterol suplerattice model. This finding is significant in that it provides a new concept in the rational design of liposomal anti-cancer drugs. More than 20 such drug formulations are in the market or under clinical trials (Immordino, et al., 2006). Most of them include cholesterol as a major component. Cholesterol is used mainly as a vesicle stabilizing agent in the original design of liposomal drugs. Our present study indicates that cholesterol is not just serving as a vesicle stabilizing agent. Actually, one can use cholesterol content to modulate the activity of liposomal drugs. The principle learned from CA4P can be extended to other liposomal anti-cancer drugs. From the membrane

biophysics point of view, this study is also significant. It provides additional data in support of the sterol superlattice model and illustrates that the concept of sterol superlattice can be applied to biotechnology development.

REFERENCES

Algire, G.H., Legallais, F.Y., Anderson, B.F., 1954. Vascular reactions of normal and malignant tissues in vivo. VI. The role of hypotension in the action of components of podophyllotoxin on transplanted sarcomas. J. Natl Cancer 14, 879-887.

Anderson, H.L., Yap, J.T., Miller, M.P., Robbins, A., Jones, T., Price, P.M., 2003. Assessment of pharmacodynamic vascular response in a phase I trial of combretastatin A4 phosphate. J. Clin. Oncol. 21, 2823-2830.

Banuo, Y., Ohai, K., Nozawa, Y., 1983. Targeting of asialofetuin sugar chain-bearing liposomes to liver lysosomes. Biochem. Int. 7, 455-459.

Boyland, E., Boyland, M.E., 1937. Studies in tissue metabolism. IX. The action of colchicine and *B. typhosus* extract. Biochem. J. 31, 454-460.

Brooks, A.C., 2003. The vascular targeting agent combretastatin A-4-phosphate induces neutrophil recruitment to endothelial cells *in vitro*. Anticancer. Res 23, 3199-3206.

Campbell, P.I., 1983. Toxicity of some charged lipids used in liposome preparation. Cytobios 37, 21-26.

Chaize, B., Colletier, J.P., 2004. Winterhalter and D. Fournier, Encapsulation of enzymes in liposomes: high encapsulation efficiency and control of

substrate permeability. Artif. Cells Blood Substit. Immobil. Biotechnol. 32, 67-75.

Chaplin, D.J., Pettit, G.R., Hill, S.A., 1999. Anti-vascular approaches to solid tumour therapy: Evaluation of combretastatin A4 phosphate. Anticancer Res 19, 189-195.

Chaplin, D.J., Pettit, G.R., Parkins, C.S., 1996. Antivascular approaches to solid tumour therapy: Evaluation of tubulin binding agents. Br J Cancer 74, 86-88.

Chong, P.L.-G., Olsher, M., 2004. Fluorescence studies of the existence and functional importance of regular distributions in liposomal membranes. Soft Materials 2, 85-108.

Chong, P.L.-G., 1996. Membrane-free volume variation with bulky lipid concentration by regular distribution: A functionally important mem. In: Markley, J.L., Northrop, D.B., Royer, C.A. (Eds.), *High-Pressure Effects in Molecular Biophysics and Enzymology*. Oxford University Press, New York, NY, 2 98-313.

Chong, P.L.-G., 1994. Evidence for regular distribution of sterols in liquid crystalline phosphatidylcholine bilayers. Proc. Natl. Acad. Sci. 91, 10069-10073.

Chong, P.L.-G., Tang, D., Sugar, I.P., 1994. Exploration of physical principles

underlying lipid regular distribution: effects of pressure, temperature, and radius of curvature on E/M dips in pyrene-labeled PC/DMPC binary mixtures. Biophys. J. 66, 2029-2038.

Chong, P.L.-G., Zhu, W., Venegas, B., 2009. On the lateral structure of model membranes containing cholesterol. Biochim. Biophys. Acta 1788, 2-11.

Chonn, A., Semple, S.C., Cullis, P.R., 1992. Association of blood proteins with large unilamellar liposomes in vivo. Relation to circulation lifetimes. J Biol Chem., 267, 18759-18765.

Damen, J., Regts, J., Scherphof, G., 1981 Transfer and exchange of phospholipid between small unilamellar liposomes and rat plasma high-density lipoproteins: dependence on cholesterol and phospholipid composition. Biochim. Biophys. Acta, 665, 538-545.

Dark, G.G., Hill, S.A., Prise, V.E., Tozer, G.M., Pettit, G.R., Chaplin, D.J., 1997a. Combretastatin A-4, an agent that displays potent and selective toxicity toward tumor vasculature. Cancer Res. 57, 1829-1834.

Dark, G.G., Hill, S.A., Prise, V.E., Tozer, G.M., Pettit, G.R., Chaplin, D.J., 1997b. Combretastatin A-4, an agent that displays potent and selective toxicity toward tumour vasculature. Cancer Res 57, 1829-1834.

Gabizon, A., Shmeeda, H., Barenholz, Y., 2003. Pharmacokinetics of

pegylated liposomal Doxorubicin: review of animal and human studies. Clin. Pharmacokinet. 42, 419-436.

Galbraith, S.M., 2001. Effects of combretastatin A4 phosphate on endothelial cell morphology *in vitro* and relationship to tumour vascular targeting activity *in vivo*. Anticancer Res. 21, 93-102.

Galbraith, S.M., Maxwell, R.J., Lodge, M.A., Tozer, G.M., Wilson, J., Taylor, N.J., Stirling, J.J., Sena, L., Padhani, A.R., Rustin, G.J., 2003. Combretastatin A4 phosphate has tumor antivascular activity in rat and man as demonstrated by dynamic magnetic resonance imaging. 21, 2831-2842.

Gregoriadis, G., Florence, A.T., 1993. Liposomes in drug delivery: Clinical, diagnostic and ophthalmic potential. Drugs 45, 15-28.

Gregoriadis, G., Neerunjun, E.D., 1975. Homing of liposomes to target cells. Biochem. Biophys. Res. Commun. 65, 537-544.

Gregoriadis, G., 1977. Targeting of drug. Nature 265, 407-411.

Grislain, L., Couvreur, P., Lenaerts, V., Roland, D.M., 1983. Depreg-Decampeneere and P. Speiser, Pharmakokinetics and distribution of a biodegradable drug-carrier. Int. J. Pharmacol. 15, 335-338.

Grosios, K., Holwell, S.E., McGown, A.T., Pettit, G.R., Bibby, M.C., 1999. In vivo and in vitro evaluation of combretastatin A-4 and its sodium phosphate

prodrug. Br. J. Cancer 81, 1318-1327.

Hashida, M., Takahashi, Y., Muranishi, S., Sezaki, H., 1977. An application of water in oil and gelatin microsphere in oil emulsions to specific delivery of anticancer agents into stomach lymphatics. J. Pharmacokin. Biopharmacol. 5, 241-244.

Hu, L.X., Li, Z.R., Wang, Y.M., Wu, Y.B., Jiang, J.D., Boykin, D.W., 2007. Novel pyridinyl and pyrimidinylcarbazole sulfonamides as antiproliferative agents. Bioorg. Med. Chem. Letters 17, 1193-1196.

Illum, L., Gones, P.D.E., Kreuker, J., Daldwin, R.W., Davis, D.D., 1983. Adsorption of monoclonal antibodies to polyhexylcyanoacrylate nanoparticles and subsequent immunospecific binding to tumor cells. Int. J. Pharm. 17, 65-69.

Immordino, M.L., Dosio, F., Cattel, L., 2006. Stealth liposomes: review of the basic science, rationale, and clinical applications, existing and potential. International Journal of Nanomedicine 1, 297-315.

Kanthou, C., Tozer, G.M., 2002. The tumor vascular targeting agent combretastatin A-4-phosphate induces reorganization of the actin cytoskeleton and early membrane blebbing in human endothelial cells. Blood 99, 2060-2069.

Koning, G.A., Kamps, J.A., Scherphof, G.L., 2002. Efficient intracellular

delivery of 5-fluorodeoxyuridine into colon cancer cells by targeted immunoliposomes. Cancer Detect. Prev. 26, 299-307.

Li, P.-., Xiao, Z., Hu, Z., Pandit, B., Sun, Y., Sackett, D.L., Werbovetz, K., Lewis, A., Johnsamuel, J., 2005. Conformationally restricted analogs of combretastatin A-4 derived from SU5416. Bioorganic & Medicinal Chemistry Letters 15, 5382-5385.

Lin, C.M., Ho, H.H., Pettit, G.R., Hamel, E., 1989. Antimitotic natural products combretastatin A-4 and combretastatin A-2: studies on the mechanism of their inhibition of the binding of colchicine to tubulin. Biochemistry 28, 6984-6991.

Lin, C.M., 1988. Interactions of tubulin with potent natural and synthetic analogs of the antimitotic agent combretastatin: a structural-activity study. Mol. Pharmacol. 34, 200-208.

Liu, F., Chong, P.L.-G., 1999. Evidence for a regulatory role of cholesterol superlattices in the hydrolytic activity of secretory phospholipase A2 in lipid membranes. Biochemistry 38, 3867-3873.

Liu, F., Sugar, I.P., Chong, P.L.-G., 1997. Cholesterol and ergosterol superlattices in three-component liquid crystalline lipid bilayers as revealed by dehydroergosterol fluorescence. Biophys. J. 72, 2243-2254.

Ludford, R.J., 1948. Factors determining the action of colchicine on tumour

growth. Br. J. Cancer 2, 75-86.

Maeda, H., Wu, J., Sawa, T., Matsumura, Y., Hori, K., 2000. Tumour vascular permeability and the EPR effect in macromolecular therapeutics: a review. J Control Release, 65, 271-284.

Mauer, N., Fenske, D.B., Cullis, P.R., 2001. Developments in liposomal drug delivery systems. Expert Opin Biol Ther, 1, 923-947.

Mayer, L.D., Dougherty, G., Harasym, T.O., Bally, M.B., 1997. The role of tumor-associated macrophages in the delivery of liposomal doxorubicin to solid murine fibrosarcoma tumors. J Pharmacol Exp Ther., 3, 1406-1414.

McGown, A.T., Fox, B.W., 1989. Structural and biochemical comparison of the anti-mitotic agents colchicine, combretastatin A4 and amphethinile. Anticancer Drug. 3, 249-254.

Mizushima, Y., Hamano, T., Yokoyama, K., 1982. Use of a lipid emulsion as a novel carrier for corticosteriods. J. Pharm. Pharmacol 34, 49-53.

Moribe, K., Maruyama, K., 2002. Pharmaceutical design of the liposomal antimicrobial agents for infectious disease. Curr. Pharm. Des. 8, 441-454.

Nallamothu, R., Wood, G.C., Pattillo, C.B., Scott, R.C., Kiani, M.F., Moore, B.M. and Thoma, L.A., 2006. A tumor vasculature targeted liposome delivery system for combretastatin A4: design, chacterization, and In vitro evaluation.

Pharm. Sci. Tech. 7, 32.

Olsher, M., Chong, P.L.-G., 2008. Sterol superlattice affects antioxidant potency and can be used to assess adverse effects of antioxidants. Anal. Biochem. 382, 1-8.

Olsher, M., Yoon, S.-.I., Chong, P.L.-.G., 2005. Role of sterol superlattice in free radical-induced sterol oxidation in lipid membranes. Biochemistry 44, 2080-2087.

Parkins, C.S., Holder, A.J., Hill, S.A., Chaplin, D.J., Tozer, G.M., 2000. Determinants of anti-vascular action by combretastatin A-4 phosphate: role of nitric oxide. Br. J. Cancer 83, 811-816.

Pattillo, C.B., Sari-Sarraf, F., Nallamothu, R., Moore, B.M., Wood, G.C., Kiani, M.F., 2005. Targeting of the antivascular drug combretastatin to irradiated tumors results in tumor growth delay. Pharm. Res. 22, 1117-1120.

Pattillo, C.B., Venegas, B., Donelson, F.J., Del Valle, L., Knight, L., Chong, P.L.-G., Kiani, M.F., 2009. Radiation-guided targeting of combretastatin encapsulated immunoliposomes to mammary tumors. Pharmaceutical Research 26, 1093-1100.

Pedley, R., Hill, S., Boxer, G., 2001. Eradication of colorectal xenografts by combined radioimmunotherapy and combretastatin A-4 3-O-phosphate. Cancer Res 61, 4716-4722.

Pettit, G.R., Cragg, G.M., Singh, S.B., 1987. Antineoplastic agents, 122. Constituents of Combretum caffrum. J. Nat. Prod 50, 386-391.

Rooijen, N., Nieuwmegen, R., 1980. Liposomes in immunology: multilamellar phosphatidylcholine liposome as a simple biodegradable and harmless adjuvant without any immunogenic activity of its own. Immunol. Commun. 9, 243-256.

Rustin, G.J.S., Galbraith, S.M., Anderson, H., Stratford, M., Folkes, L.K., Sena, L., Gumbrell, L., Price, P.M., 2003. Phase I clinical trial of weekly combretastatin A4 phosphate: clinical and pharmacokinetic results. J. Clin. Oncol. 21, 2815-2822.

Sapra, P., Tyagi, P., Allen, T.M., 2005. Ligand-targeted liposomes for cancertreatment. Curr Drug Deliv., 2, 369-381.

Seed, L., Slaughter, D.P., Limarzi, L.R., 1940. Effect of colchicine on human carcinoma. Surgery 7, 696-709.

Senior, J., 1982. Is half-life of circulating liposomes determined by changes in their permeability? FEBS Lett., 145, 109-114.

Soriano, P., Dijkstra, J., Legrand, A., Spanjer, H., Gagliardi, D., Roerdink, F., Scherphof, G., C, N., 1983. Targeted and non-targeted liposomes for in vivo transfer to rat liver cells of a plasmid containing the preproinsulin I gene. Proc. Natl. Acad. Sci. USA 80, 7128-7131.

Stevenson, J.P., Rosen, M., Sun, W., Gallagher, M., Haller, D.G., Vaughn, D., Giantonio, B., Zimmer, R., Petros, W.P., Stratford, M., Chaplin, D., Young, S.L., Schnall, M., ODwyer , P.J., 2003. Phase I trial of the antivascular agent combretastatin A4 phosphate on a 5-day schedule to patients with cancer: magnetic resonance imaging evidence for altered tumor blood flow. J. Clin. Oncol. 21, 4428-4438.

Straubinger, R., Duzgunes, N., Papahadjopoulus, D., 1985. pH-sensitive liposomes mediate cytoplasmic delivery of encapsulated macromolecules. FEBS Letters, 179, 148-154.

Tang, D., Chong, P.L.-G., 1992. E/M dips. Evidence for lipids regularly distributed into hexagonal super-lattices in pyrene-PC/DMPC binary mixtures at specific concentrations. Biophys. J. 63, 903-910.

Tozer, G.M., 2001. Mechanisms associated with tumor vascular shutdown induced by combretastatin A-4 phosphate: intravital microscopy and measurement of vascular permeability. Cancer Res. 61, 6413-6422.

Tozer, G.M., Prise, V.E., Wilson, J., Locke, R.J., Vojnovic, B., Stratford, M.R., Dennis, M.F., Chaplin, D.J., 1999. Combretastatin A-4 phosphate as a tumor vascular-targeting agent: early effects in tumors and normal tissues. Cancer Res. 59, 1626-1634.

Venegas, B., Sugar, I.P., Chong, P.L.-G., 2007. Critical factors for detection

of biphasic changes in membrane properties at specific sterol mole fractions for maximal superlattice formation. J. Phys. Chem. B. 111, 5180-5192.

Vincent, L., Kermani, P., Young, M.L., Cheng, J., Zhang, F., Shido, K., Lam, G., Bompais-Vincent, H., Zhu, Z., Hicklin, D.J., Bohlen, P., Chaplin, D.J., May, C., Rafii, S., 2005. Combretastatin A4 phosphate induces rapid regression of tumor neovessels and growth through interference with vascular endothelial-cadherin signaling. J. Clin. Invest. 115, 2992-3006.

Virtanen, J.A., Somerharju, P., Kinnunen, P.K.J., 1988. Prediction of patterns for the regular distribution of soluted guest molecules in liquid crystalline phospholipid membranes. J. Mol. Electron 4, 233-236.

Wang, M.M., Olsher, M., Sugar, I.P., Chong, P.L.-G., 2004. Cholesterol superlattice modulates the activity of cholesterol oxidase in lipid membranes. Biochemistry 43, 2159-2166.

Wang, M.M., Sugar, I.P., Chong, P.L.-G., 1998. Role of the sterol superlattice in the partitioning of the antifungal drug nystatin into lipid membranes. Biochemistry 37, 11797-11805.

Weissmann, G., Bloomgerden, D., Kaplan, R., Cohen, C., Hoffstein, S., Collins, T., Gotlieb, A.D., 1975. A general method for introduction of enzymes, by means of immunoglobulin coated liposomes into lysosomes of deficient ceLLS. Proc. Natl. Acad. Sci. 72, 88-94.

Wu, P.S., Wu, H.M., Tin, G.W., Schuh, J.R., Croasmun, W.R., Baldeschwieler, J.D., Shen, T. Y. M. M. Pompipom, 1982. Stability of carbohydrate-modified vesicles in vivo: comparative effect of ceramide and cholesterol glycoconjugates. Proc. Natl. Acad. Sci. USA 79, 5490-5493.

Zhao, D., Jiang, L., Hahn, E., Mason, R.P., 2005. Tumor physiological response to combretastatin A4 phosphate assessed by MRI. Int. J. Radiat. Oncol. Biol. Phys., 62, 872-880.